

# The topology of Liouville foliation for the Kovalevskaya integrable case on the Lie algebra $\mathfrak{so}(4)$ .

Kozlov I. K.\*  
ikozlov90@gmail.com

## Abstract

In this paper we study topological properties of an integrable case for Euler's equations on the Lie algebra  $\mathfrak{so}(4)$ , which can be regarded as an analogue of the classical Kovalevskaya case in rigid body dynamics. In particular, for all values of the parameters of the system under consideration the bifurcation diagrams of the momentum mapping are constructed, the types of critical points of rank 0 are determined, the bifurcations of Liouville tori are described and the loop molecules for all singular points of the bifurcation diagram are computed. It follows from the obtained results that some topological properties of the classical Kovalevskaya case can be obtained from the corresponding properties of the considered integrable case on the Lie algebra  $\mathfrak{so}(4)$  by taking a natural limit.

Bibliography: 21 titles.

**Keywords:** integrable Hamiltonian systems, Kovalevskaya case, Liouville foliation, bifurcation diagram, topological invariants.

## Contents

<b>1</b>	<b>Introduction</b>	<b>2</b>
<b>2</b>	<b>Basic Definitions and Problem Formulation</b>	<b>3</b>
<b>3</b>	<b>Main results</b>	<b>6</b>
3.1	Case $\varkappa > 0, b = 0$ . . . . .	16

---

\*No Affiliation, Moscow, Russia.

<sup>0</sup>This work was supported by the Russian Foundation for Basic Research (grant nos. 13-01-00664-a and 12-01-31497), the programme "Leading Scientific Schools" (grant no. HIII-581.2014.1) and a grant from the Government of the Russian Federation for the State Support of Research at Russian Institutes of Higher Education Supervised by Leading Scientists (contract no. 11.G34.31.0054).

<b>4</b>	<b>Proof of the main statements</b>	<b>20</b>
4.1	Critical points of rank 1 . . . . .	20
4.2	Types of bifurcation diagrams. (Case $b \neq 0$ ) . . . . .	26
4.3	Critical points of rank 0 . . . . .	30
4.4	Proof of Theorems 1, 2 and 3 . . . . .	34
<b>5</b>	<b>Classical Kovalevskaya case (<math>\varkappa = 0</math>)</b>	<b>37</b>

# 1 Introduction

The Kovalevskaya top is one of the most well-known integrable Hamiltonian systems in classical mechanics. It was proved by Sofia Kovalevskaya in her paper [1] that besides the cases of Euler, Lagrange and her own, opened earlier in [2], there is no other rigid body systems that would be integrable in the same way for any value of the area constant. The Kovalevskaya top is more complex than the Euler and Lagrange tops hence various methods that would allow us to simplify the work with this top are of interest. In this paper we demonstrate one of such possible methods. Namely, we consider a one-parameter family of integrable Hamiltonian systems defined on the pencil of Lie algebras  $\mathfrak{so}(4) - \mathfrak{e}(3) - \mathfrak{so}(3, 1)$  found in the paper [3] and show that some information about the classical Kovalevskaya case, which is an integrable Hamiltonian system on the Lie algebra  $\mathfrak{e}(3)$ , can be obtained by studying the integrable Hamiltonian systems on the Lie algebra  $\mathfrak{so}(4)$ . To be more precise, in this paper we calculate some topological invariants of these integrable cases using the theory of topological classification of integrable Hamiltonian systems (see [4]). The obtained results for the Lie algebra  $\mathfrak{so}(4)$  allow us to make some conclusions about the topological properties of the classical Kovalevskaya case.

In this paper for the integrable cases on the algebra  $\mathfrak{so}(4)$  under consideration it is done the following:

1. the bifurcation diagrams of the momentum mapping are constructed (Theorem 1),
2. the types of critical points of rank 0 are determined (Lemma 2),
3. the bifurcations of Liouville tori are described (Theorem 2) and the loop molecules for all singular points of the bifurcation diagram are computed (Theorem 3).

Using the results of this paper it is not hard to obtain the classification of isoenergetic surfaces up to the rough Liouville equivalence. In other words, for each isoenergetic surface  $H = \text{const}$  it is not hard to construct the corresponding unmarked molecule (the Fomenko invariant). We do not do it in this paper because the description of all possible molecules would be rather cumbersome. The molecules depend not only on the type of bifurcation diagrams, but also on the value of the Hamiltonian at the critical points of rank 0. The knowledge of loop molecules also allows us to easily restore a number of marks for these rough molecules. Recall that the marked molecules (the Fomenko–Zieschang invariants) are important topological invariants of integrable

Hamiltonian systems, which completely describe the structure of the Liouville foliation on non-singular three-dimensional isoenergetic surfaces. Namely, the Fomenko–Zieschang theorem states that two integrable Hamiltonian systems on two isoenergetic surfaces are Liouville equivalent (that is, there exists a diffeomorphism taking one Liouville foliation to another) if and only if their marked molecules coincide (for more details about the Fomenko–Zieschang invariants see, for example, [4]).

The idea to consider integrable Hamiltonian systems on compact Lie algebras can become fruitful: the coadjoint orbits of compact Lie algebras are compact which greatly simplifies the analysis of integrable Hamiltonian systems on them. For example, in the case under consideration, since the orbits are compact, for the construction of bifurcation diagrams and the calculation of loop molecules it suffices to find the curves that contain the image of critical points and find the types of critical points of rank 0. Earlier integrable Hamiltonian systems on the Lie algebra  $\mathfrak{so}(4)$  were studied in the papers [5] (compact analogue of the Clebsch case), [6] (the Sokolov case) and [7] (compact analogue of the Steklov case). Let us also note that algebraic and topological properties of integrable systems related to the Lie algebra  $\mathfrak{so}(4)$  and other compact Lie algebras were studied in [8] and [9].

The topology of the classical Kovalevskaya case was studied in detail in the book [10] (see also [11] and [12]). In particular, in this book the bifurcation diagrams of the momentum mapping and the bifurcations of Liouville tori for the critical values of the momentum mapping are described. The loop molecules (as well as fine Liouville classification) for the classical case Kovalevskaya are contained in the paper [13]. All necessary results on the classical Kovalevskaya case are collected in a convenient form in the book [4]. The connection between the classical Kovalevskaya case and the considered in this paper system on the Lie algebra  $\mathfrak{so}(4)$  is discussed in Section 5.

The case of the zero area constant ( $b = 0$ ) was described earlier in the paper [14].

## 2 Basic Definitions and Problem Formulation

Recall that there exists a natural linear Poisson bracket on the dual space  $\mathfrak{g}^*$  to any finite-dimensional Lie algebra  $\mathfrak{g}$  given by the formula

$$\{f, g\} = \langle x, [df|_x, dg|_x] \rangle. \quad (1)$$

Here  $\langle \cdot, \cdot \rangle$  denotes the value of the covector in  $\mathfrak{g}^*$  on a vector in  $\mathfrak{g}$ , and  $[\cdot, \cdot]$  denotes the commutator in the Lie algebra  $\mathfrak{g}$ . In the formula (1) we use the canonical isomorphism  $(\mathfrak{g}^*)^* = \mathfrak{g}$ . The bracket (1) is called the Lie-Poisson bracket.

DEFINITION 1. Let  $\mathfrak{g}$  be a finite-dimensional Lie algebra,  $x_1, \dots, x_n$  be linear coordinates in the dual space  $\mathfrak{g}^*$ , and  $H$  be a smooth function on  $\mathfrak{g}^*$ . The equations

$$\dot{x}_i = \{x_i, H\}, \quad (2)$$

which define a dynamical system on  $\mathfrak{g}^*$ , are called *Euler's equations* for the Lie algebra  $\mathfrak{g}$ .

It is well-known (see, for example, [4]), that the classical Kovalevskaya case can be defined by Euler's equations on the Lie algebra  $\mathfrak{e}(3)$ . It turns out that the classical Kovalevskaya case can be included in a one-parameter family of integrable systems defined on the pencil of Lie algebras  $\mathfrak{so}(4) - \mathfrak{e}(3) - \mathfrak{so}(3, 1)$ .

Consider the six-dimensional space  $\mathbb{R}^6$  and fix a basis  $e_1, e_2, e_3, f_1, f_2, f_3$  in it. Consider the following one-parameter family of commutators in  $\mathbb{R}^6$  depending on the parameter  $\varkappa \in \mathbb{R}$ :

$$[e_i, e_j] = \varepsilon_{ijk} e_k, \quad [e_i, f_j] = \varepsilon_{ijk} f_k, \quad [f_i, f_j] = \varkappa \varepsilon_{ijk} e_k, \quad (3)$$

where  $\varepsilon_{ijk}$  is the sign of the permutation  $\{123\} \rightarrow \{ijk\}$ . It is easy to check that the cases  $\varkappa > 0$ ,  $\varkappa = 0$  and  $\varkappa < 0$  correspond to the Lie algebras  $\mathfrak{so}(4)$ ,  $\mathfrak{e}(3)$  and  $\mathfrak{so}(3, 1)$  respectively.

In the coordinates  $J_1, J_2, J_3, x_1, x_2, x_3$  on the dual linear space corresponding to the basis  $e_1, e_2, e_3, f_1, f_2, f_3$  the Lie-Poisson bracket has a similar form

$$\{J_i, J_j\} = \varepsilon_{ijk} J_k, \quad \{J_i, x_j\} = \varepsilon_{ijk} x_k, \quad \{x_i, x_j\} = \varkappa \varepsilon_{ijk} J_k. \quad (4)$$

For any value of the parameter  $\varkappa \in \mathbb{R}$  the bracket (4) has two Casimir functions:

$$f_1 = \mathbf{x}^2 + \varkappa \mathbf{J}^2, \quad f_2 = \langle \mathbf{x}, \mathbf{J} \rangle, \quad (5)$$

where  $\mathbf{x}$  and  $\mathbf{J}$  denote the three-dimensional vectors  $(x_1, x_2, x_3)$  and  $(J_1, J_2, J_3)$  respectively and  $\langle \cdot, \cdot \rangle$  denotes the Euclidean scalar product of two vectors in  $\mathbb{R}^3$ . Recall that functions are called Casimir functions of a Poisson bracket if they commute with any other function with respect to this bracket. The joint level surfaces

$$M_{a,b} = \{(\mathbf{J}, \mathbf{x}) \mid f_1(\mathbf{J}, \mathbf{x}) = a, \quad f_2(\mathbf{J}, \mathbf{x}) = b\} \quad (6)$$

are the orbits of the coadjoint representation except for the case  $\varkappa \leq 0, a = 0, b = 0$  (in this case, the level surface is a union of several orbits of the coadjoint representation). In all other cases the surfaces  $M_{a,b}$  are symplectic leaves of the bracket (4), in particular, the bracket (4) defines a symplectic structure on them. If  $\varkappa > 0$  and  $a > 2\sqrt{\varkappa}|b|$ , then the orbits  $M_{a,b}$  are four-dimensional submanifolds of  $\mathbb{R}^6(\mathbf{J}, \mathbf{x})$  diffeomorphic to the product of two two-dimensional spheres  $\mathbb{S}^2 \times \mathbb{S}^2$ . If  $\varkappa > 0$ , then the singular orbits  $a = 2\sqrt{\varkappa}|b|$  are diffeomorphic to the two-dimensional sphere  $\mathbb{S}^2$ . If  $\varkappa > 0$ , then there is no orbits satisfying the condition  $a < 2\sqrt{\varkappa}|b|$ . Let us also note that if  $\varkappa = 0$ , then the non-singular orbits  $a > 0$  are diffeomorphic to the cotangent bundle of the two-dimensional sphere  $T^*\mathbb{S}^2$  (in particular, they are not compact).

In this paper we examine the following integrable case for Euler's equations defined on the pencil of Lie algebras  $\mathfrak{so}(4) - \mathfrak{e}(3) - \mathfrak{so}(3, 1)$  described above (see, for example, [3] or [15]). In the coordinates  $(J_i, x_j)$  described above the Hamiltonian is equal to

$$H = J_1^2 + J_2^2 + 2J_3^2 + 2c_1 x_1 \quad (7)$$

and the integral has the form

$$K = (J_1^2 - J_2^2 - 2c_1 x_1 + \varkappa c_1^2)^2 + (2J_1 J_2 - 2c_1 x_2)^2, \quad (8)$$

where  $c_1$  is an arbitrary constant.

Note that without loss of generality we may assume that  $c_1 = 1$  and  $\varkappa = -1, 0$  or  $1$  since the change of coordinates and parameters of the system given by the formulas

$$J' = \mu J, \quad x' = \lambda \mu x, \quad a' = \mu^2 \lambda^2 a, \quad b' = \mu^2 \lambda b, \quad c'_1 = \frac{\mu}{\lambda} c_1, \quad \varkappa' = \lambda^2 \varkappa,$$

where  $\lambda, \mu$  are arbitrary constants, multiplies the Hamiltonian and the integral by  $\mu^2$  and  $\mu^4$  respectively. Nevertheless we will preserve both  $c_1$  and  $\varkappa$  in order to get “homogeneous” formulas (for example, the Hamiltonian and the integral are homogeneous functions of  $\mathbf{J}, \mathbf{x}, c_1$ ).

REMARK 1. It is not hard to verify that if  $\varkappa = 0$  (and  $c_1 = 1$ ), then we obtain the classical Kovalevskaya case in the form in which it was described, for example, in the book [4]. More precisely, in the book [4] the Hamiltonian is 2 times less than the Hamiltonian (7) and the first integral is 4 times less than the integral (8). Note also that in the book [4] the following notation is used:  $S_i = J_i, R_j = x_j$ , the value  $b$  of the integral  $f_2$  is denoted by  $g$  and the value  $a$  of the integral  $f_1$  is assumed to be equal to 1.

REMARK 2. The change of coordinates  $(\mathbf{J}, \mathbf{x}) \rightarrow (-\mathbf{J}, \mathbf{x})$  preserves the integral  $f_1$ , the Hamiltonian (7) and the integral (8) whereas it changes the sign of the integral  $f_2$ . Therefore, without loss of generality, we can assume that  $b \geq 0$ .

REMARK 3. Note also that the system has the following two natural symmetries that preserve the Hamiltonian (7), the first integral (8) and both integral  $f_1$  and  $f_2$ . The first symmetry  $\sigma_2$  changes the signs of the coordinates  $J_2$  and  $x_2$  and preserves the remaining coordinates:

$$\sigma_2 : (J_1, J_2, J_3, x_1, x_2, x_3) \rightarrow (J_1, -J_2, J_3, x_1, -x_2, x_3).$$

Similarly, the second symmetry  $\sigma_3$  simultaneously changes the signs of the coordinates  $J_3$  and  $x_3$ :

$$\sigma_3 : (J_1, J_2, J_3, x_1, x_2, x_3) \rightarrow (J_1, J_2, -J_3, x_1, x_2, -x_3).$$

Further we construct the bifurcation diagrams of the momentum mapping, determine the types of critical points, describe the bifurcations of Liouville tori and calculate the loop molecules for singular points of the bifurcation diagrams for the given Hamiltonian systems with Hamiltonian (7) and integral (8) on non-singular orbits  $M_{a,b}$ . We use some facts and notation from the theory of topological classification developed by A. T. Fomenko and his disciples. The definitions of topological invariants (atoms, molecules) as well as the basic facts about this theory can be found in the book [4]. For various applications of this theory in rigid body dynamics see, for example, [16]. Let us also note that this theory has recently played an important role in the study of symmetries of Liouville tori bifurcations and in the construction of a classification theory for such symmetries (see [17], [18], [19] and [20]).

In this paper we only briefly recall the idea of the method of loop molecules. A smooth curve without self-intersections in the plane  $\mathbb{R}^2(H, K)$  is called admissible if it intersects the bifurcation diagram transversally and does not pass through its singular

points. The preimage of any admissible curve is a three-dimensional manifold equipped with a Liouville foliation. An invariant of this foliation is a marked molecule, which is a graph whose edges correspond to the one-parameter families of Liouville tori and whose vertices correspond to the singular leaves of this foliation. Symbols are placed in the vertices of the graph which specify the types of the bifurcations. In addition the graph is endowed, in a certain way, with three types of marks ( $r$ ,  $\epsilon$  and  $n$ ), which indicate the relation between different bifurcations. The loop molecule of a singular point  $x$  of a bifurcation diagram is the marked molecule that describes the Liouville foliation in the preimage of any sufficiently small admissible closed curve surrounding the point  $x$ . Loop molecules can provide information about different molecules of admissible curves (for example, sometimes molecules of curves can be “glued” together from parts of loop molecules). Examples of loop molecules are given in Tables 2 and 3.

### 3 Main results

We now state the main results. First, we describe the results for the case  $b \neq 0$  and then for the case  $b = 0$ . Let us start with the description of the bifurcation diagrams of the momentum mapping.

LEMMA 1. *Let  $b \neq 0$  and  $\varkappa \neq 0$ . Then for any non-singular orbit  $M_{a,b}$  (that is, for any orbit such that  $a^2 - 4\varkappa b^2 \neq 0$ ) the bifurcation diagram  $\Sigma_{h,k}$  for the integrable Hamiltonian system with Hamiltonian (7) and integral (8) is contained in the union of the following three families of curves on the plane  $\mathbb{R}^2(h, k)$ :*

1. *The line  $k = 0$ ;*
2. *The parametric curve*

$$h(z) = \frac{b^2 c_1^2}{z^2} + 2z, \quad k(z) = \left( 4ac_1^2 - \frac{4b^2 c_1^2}{z} + \frac{b^4 c_1^4}{z^4} \right) - 2\varkappa c_1^2 h(z) + \varkappa^2 c_1^4, \quad (9)$$

where  $z \in \mathbb{R} - \{0\}$ .

3. *The union of two parabolas*

$$k = \left( h - \varkappa c_1^2 - \frac{a}{\varkappa} + \frac{\sqrt{a^2 - 4\varkappa b^2}}{\varkappa} \right)^2 \quad (10)$$

and

$$k = \left( h - \varkappa c_1^2 - \frac{a}{\varkappa} - \frac{\sqrt{a^2 - 4\varkappa b^2}}{\varkappa} \right)^2. \quad (11)$$

The proof of Lemma 1 is given in Section 4.1.

In order to construct the bifurcation diagrams of the momentum mapping it remains to throw away several parts of the curves described in Lemma 1. The precise description of the bifurcation diagrams is given in the following theorem.

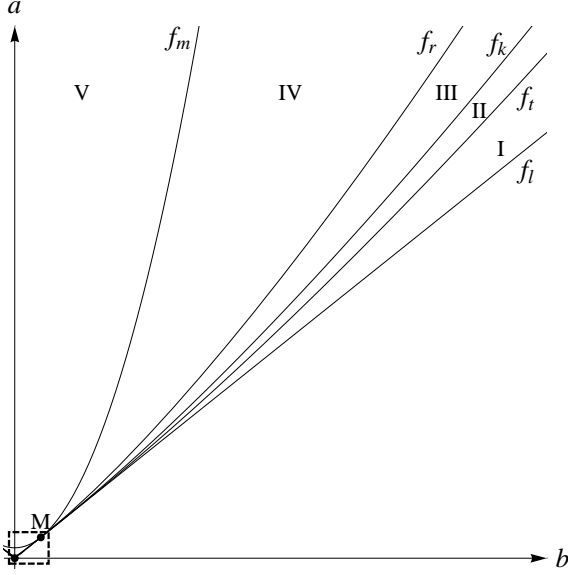


Figure 1: Partition of the set of parameters

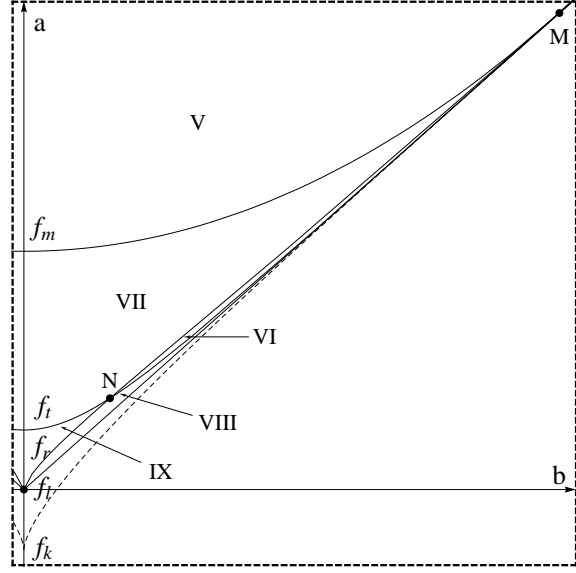


Figure 2: An enlarged fragment of Fig. 1

**THEOREM 1.** *Let  $\varkappa > 0$  and  $b > 0$ . Then the functions  $f_k, f_r, f_m, f_t$  and  $f_l$  given by the formulas*

$$f_k(b) = \frac{3b^{4/3} + 6\varkappa b^{2/3} c_1^{4/3} - \varkappa^2 c_1^{8/3}}{4c_1^{2/3}} \quad (12)$$

$$f_r(b) = \frac{b^{4/3}}{c_1^{2/3}} + \varkappa b^{2/3} c_1^{2/3} \quad (13)$$

$$f_m(b) = \frac{b^2}{\varkappa c_1^2} + \varkappa^2 c_1^2 \quad (14)$$

$$f_t(b) = \left( \frac{\varkappa c_1^2 + t^2}{2c_1} \right)^2 + \varkappa t^2, \quad \text{where } b = t \left( \frac{\varkappa c_1^2 + t^2}{2c_1} \right) \quad (15)$$

$$f_l(b) = 2\sqrt{\varkappa}|b| \quad (16)$$

divide the area  $\{b > 0, a > 2\sqrt{\varkappa}b\} \subset \mathbb{R}^2(a, b)$  into 9 areas (see Fig. 1 and 2). In Fig. 3 – 21 the corresponding bifurcation diagrams of the momentum mapping for the integrable Hamiltonian system with Hamiltonian (7) and integral (8) on the orbit  $M_{a,b}$  of the Lie algebra  $so(4)$  are shown for each of these areas. More precisely, in each case it is specified from which parts of the line  $k = 0$ , the curve (9) and two parabolas (10) and (11) the bifurcation diagram of the momentum mapping is composed.

Recall that the bifurcation diagram for an orbit  $M_{a,b}$  with  $b < 0$  coincides with the bifurcation diagram for the orbit  $M_{a,-b}$  (see Remark 2).

**REMARK 4.** In Fig. 3 – 21 the arcs  $y_8 z_2, z_2 z_1, y_5 z_3, z_8 z_9, z_8 z_{11}$  and  $z_9 z_{11}$  belong to the parametric curve (9). The rest of the arcs of the bifurcation diagrams distribute between the curves in an obvious way.

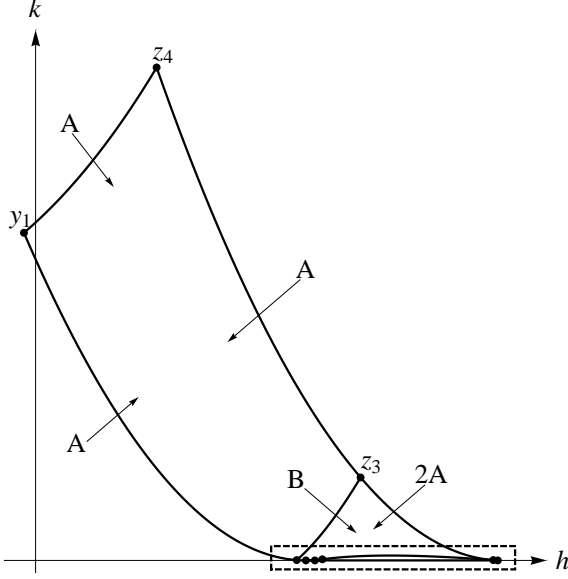


Figure 3: Area I:  $\varkappa^3 c_1^4 < b^2$ ,  $f_l(b) < a < f_t(b)$

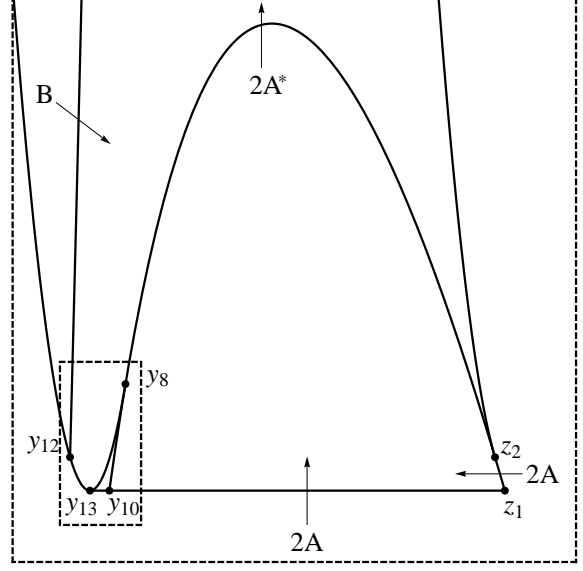


Figure 4: Area I: an enlarged fragment of Fig. 3

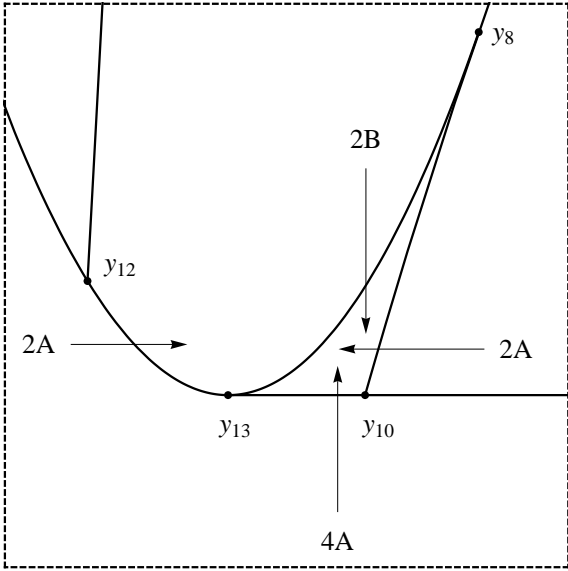


Figure 5: Area I: an enlarged fragment of Fig. 4

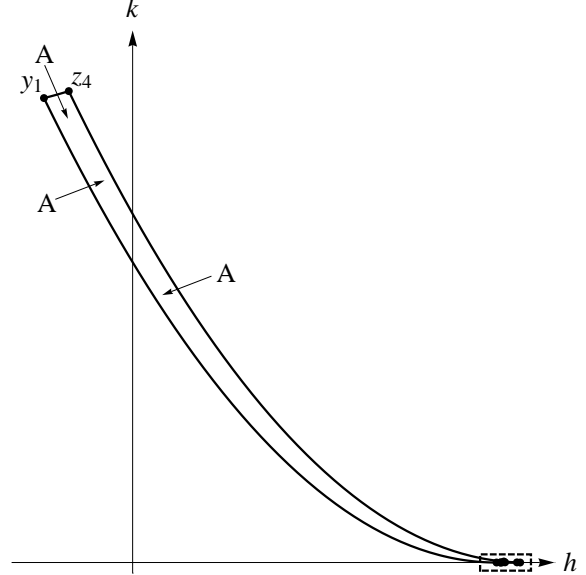


Figure 6: Area II:  $\varkappa^3 c_1^4 < b^2$ ,  $f_t(b) < a < f_k(b)$

REMARK 5. In this paper 9 areas of the plane  $\mathbb{R}^2(a, b)$  are numbered with Roman numerals I–IX as it is shown in Fig. 1 and 2 (the relative positioning of the graphs of functions  $f_k, f_r, f_m, f_t$  and  $f_l$  is also described in Assertion 14). We continue the numbering on the areas of the line  $b = 0$  as follows:

- area X:  $\{b = 0, \varkappa^2 c_1^2 < a\}$ ;
- area XI:  $\{b = 0, \frac{\varkappa^2 c_1^2}{4} < a < \varkappa^2 c_1^2\}$ ;

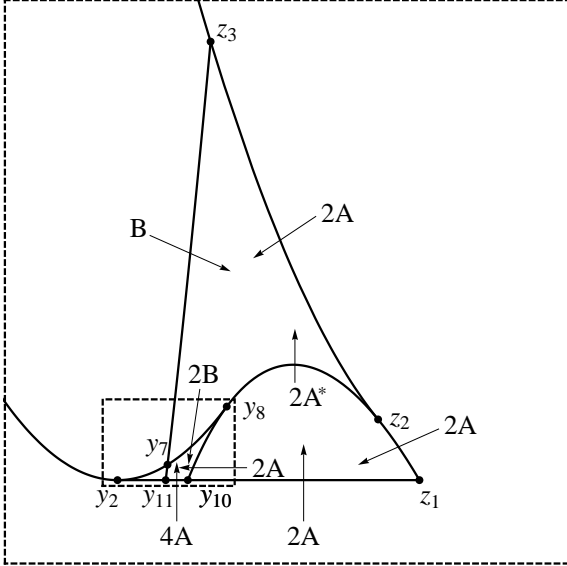


Figure 7: Area II: an enlarged fragment of Fig. 6

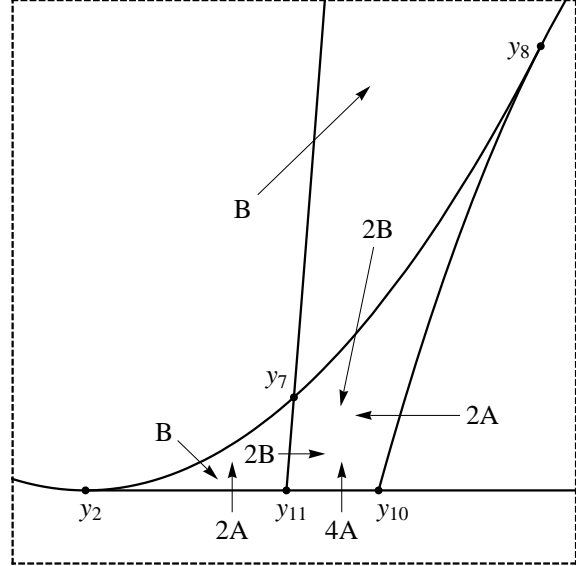


Figure 8: Area II: an enlarged fragment of Fig. 7

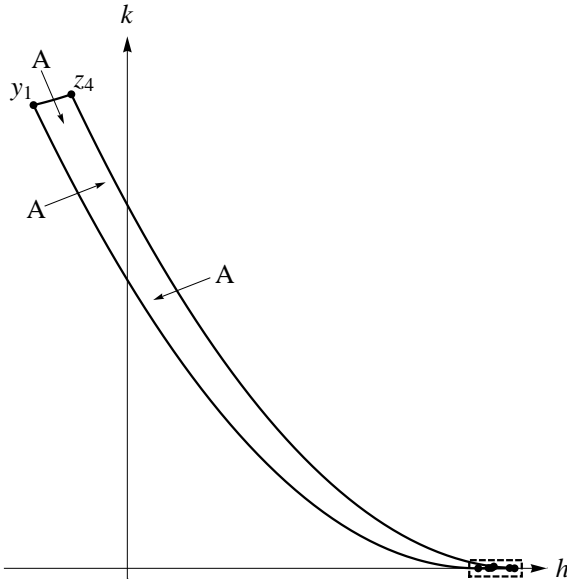


Figure 9: Area III:  $\varkappa^3 c_1^4 < b^2$ ,  $f_k(b) < a < f_r(b)$

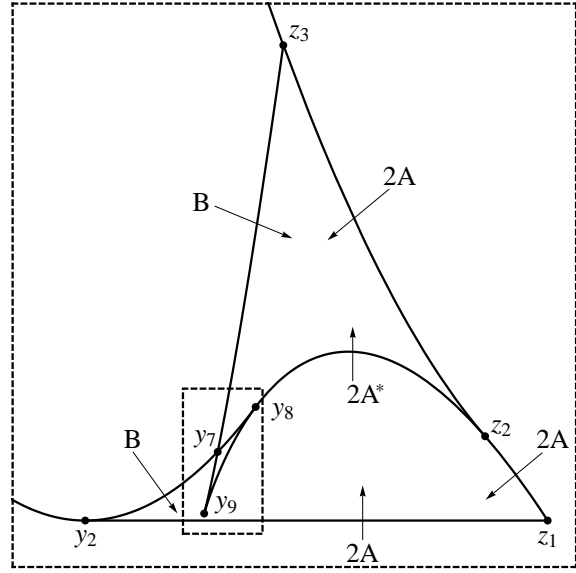


Figure 10: Area III: an enlarged fragment of Fig. 9

- area XII:  $\{b = 0, \quad 0 < a < \frac{\varkappa^2 c_1^2}{4}\}$ ;

A detailed description of the relative positioning of the curves that contain the bifurcation diagrams of the momentum mapping are given in Section 4.2. The proof of Theorem 1 is given in Section 4.4. In fact, in order to prove Theorem 1 it suffices to know the types of critical points of rank 0, which are described in the following lemma (for the definition of nondegenerate critical points of rank 0 and their types see, for example, [4]).

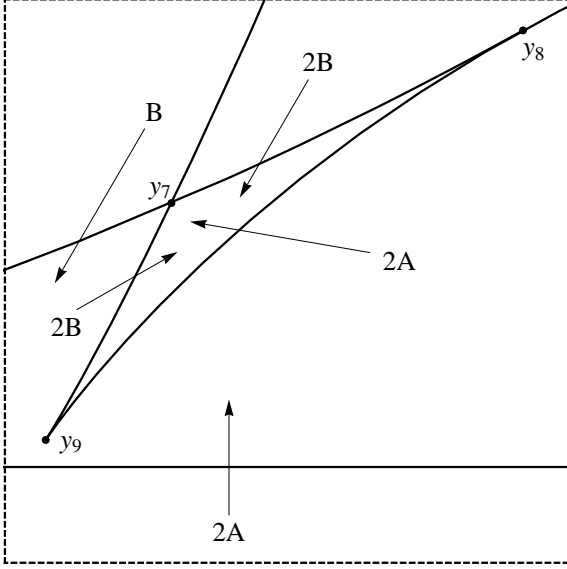


Figure 11: Area III: an enlarged fragment of Fig.10

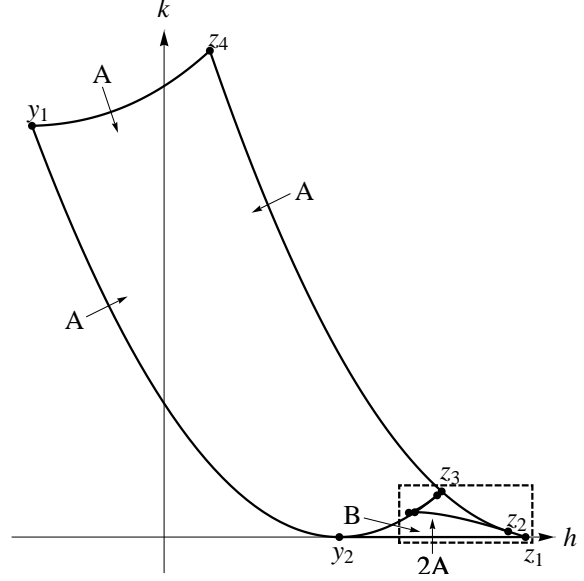


Figure 12: Area IV:  $\varkappa^3 c_1^4 < b^2$ ,  $f_r(b) < a < f_m(b)$

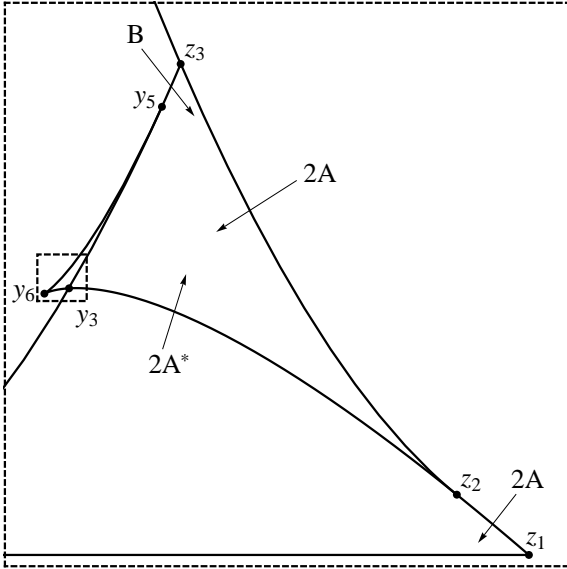


Figure 13: Area IV: an enlarged fragment of Fig. 12

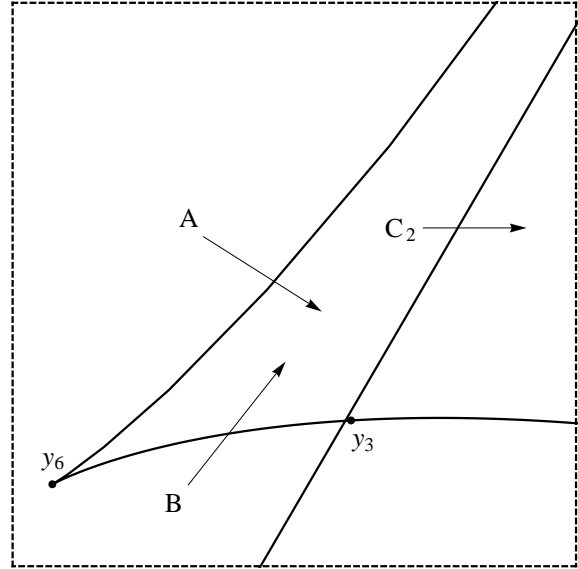


Figure 14: Area IV: an enlarged fragment of Fig.13

LEMMA 2. Let  $\varkappa > 0$  and  $b > 0$ . Then the image of critical points of rank 0 is contained in the union of the following three families of points.

1. The point of intersection of the parabolas (10) and (11) (the point  $z_5$  in Fig. 15). It has coordinates

$$h = \varkappa c_1^2 + \frac{a}{\varkappa}, \quad k = \frac{a^2 - 4\varkappa b^2}{\varkappa^2}.$$

If  $a > f_m(b)$ , where the function  $f_m(b)$  is given by the formula (14), then there

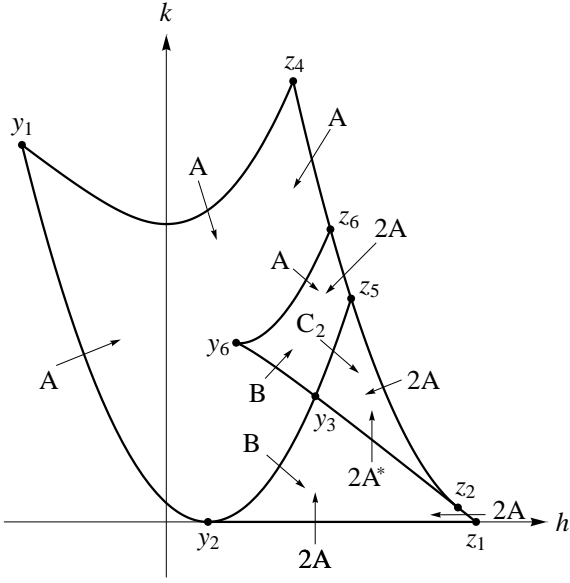


Figure 15: Area V:  $f_m(b) < a$

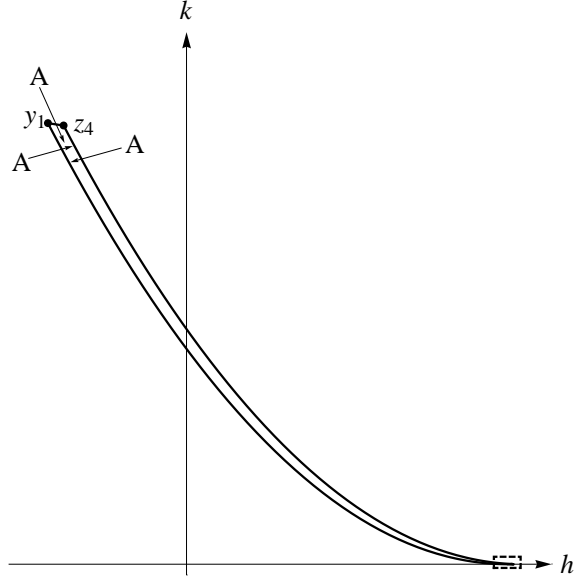


Figure 16: Area VI:  $0 < b^2 < \varkappa^3 c_1^4$ ,  $f_t(b) < a < f_r(b)$

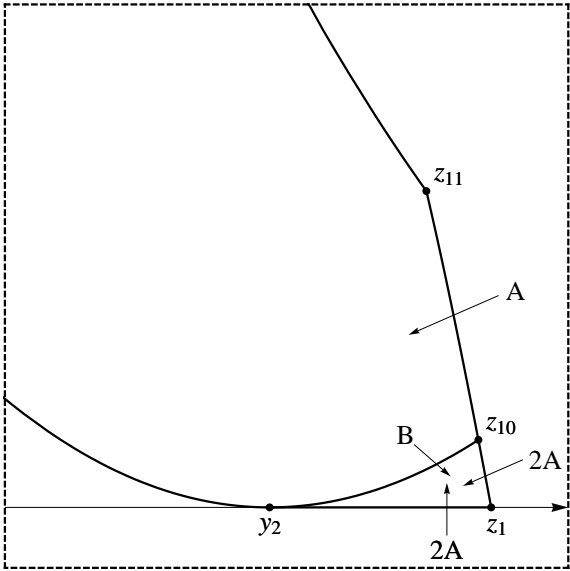


Figure 17: Area VI: an enlarged fragment of Fig.16

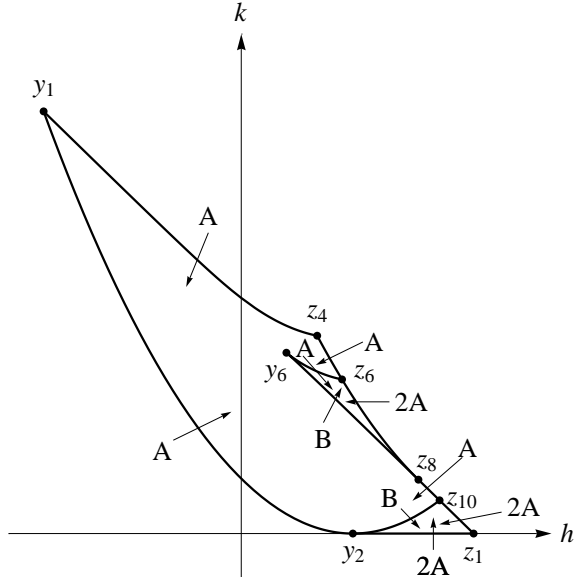


Figure 18: Area VII:  $0 < b^2 < \varkappa^3 c_1^4$ ,  $\max(f_t(b), f_r(b)) < a < f_m(b)$

are two critical points of rank 0 in the preimage of the point on the orbit  $M_{a,b}$ . If  $a = f_m(b)$ , then there is one critical point of rank 0 in the preimage and if  $a < f_m(b)$ , then there is no critical points of rank 0 in the preimage. If  $a > f_m(b)$ , then all critical points from this series are nondegenerate critical points of saddle-center type.

2. The point of intersection of the parabolas (10), (11) and the curve (9). The

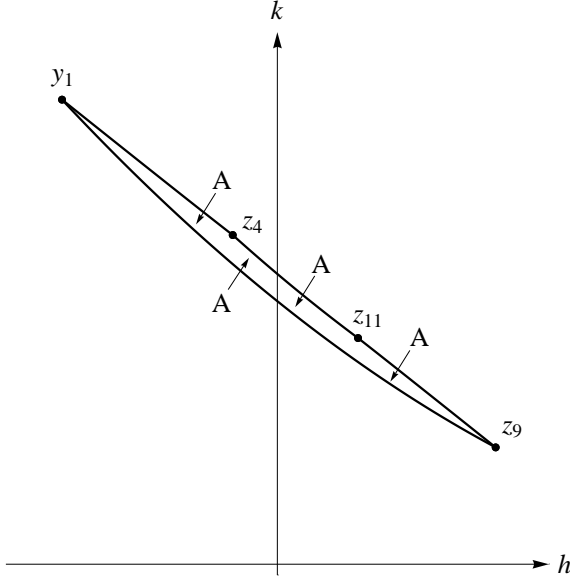


Figure 19: Area VIII:  $0 < b^2 < z^3 c_1^4$ ,  $f_l(b) < a < \min(f_r(b), f_t(b))$

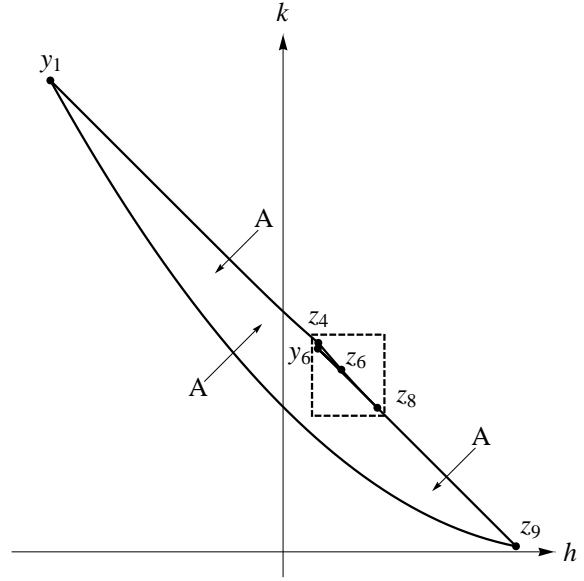


Figure 20: Area IX:  $0 < b^2 < z^3 c_1^4$ ,  $f_r(b) < a < f_t(b)$

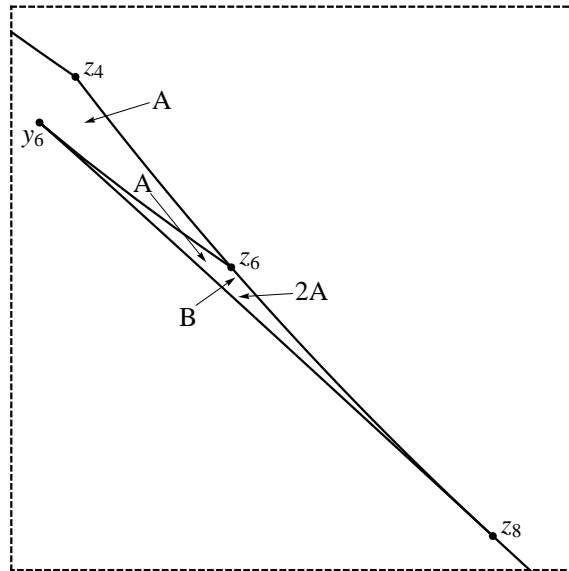


Figure 21: Area IX: an enlarged fragment of Fig. 20

corresponding values of the parameter  $z$  of the curve (9) are given by the equation

$$z^2 = \frac{a \pm \sqrt{a^2 - 4zb^2}}{2} c_1^2.$$

For each non-singular orbit  $M_{a,b}$  there is exactly one critical point of rank 0 in the preimage of each intersection point of the curve (9) with the parabolas. Both critical points such that  $z < 0$  (that is the points  $y_1$  and  $z_4$  in Fig. 3–25) have center-center type.

The types of the remaining points are given in Table 1. Here  $z_{+l}$  and  $z_{+r}$  are the remaining points of intersection of the curve (9) with the left parabola (10) and the right parabola (11) respectively and the functions  $f_r(b)$ ,  $f_m(b)$  and  $f_t(b)$  are given by the formulas (13), (14) and (15) respectively. (In Fig. 3–21 the point  $z_{+r}$  is denoted by  $z_3$ ,  $z_6$  or  $z_{11}$  depending on the type of the point. The point  $z_{+l}$  is denoted by  $y_3$ ,  $y_7$ ,  $y_{12}$ ,  $z_9$  or  $z_{10}$ .)

		$0 < b^2 < \varkappa^3 c_1^4$	$b^2 > \varkappa^3 c_1^4$
$a > f_m(b)$	$z_{+r}$	center-center	center-center
	$z_{+l}$	saddle-saddle	saddle-saddle
$f_m(b) > a > f_t(b)$ $a \neq f_r(b)$	$z_{+r}$	center-center	center-saddle
	$z_{+l}$	center-saddle	saddle-saddle
$f_t(b) > a > f_l(b)$ $a \neq f_r(b)$	$z_{+r}$	center-center	center-saddle
	$z_{+l}$	center-center	center-saddle

Table 1: Types of intersections of the curve (9) and the parabolas (10) and (11).

3. The points of intersection of the curve (9) and the line  $k = 0$  (the points  $y_{10}$ ,  $y_{11}$  and  $z_1$  in Fig. 3–21). In the preimage of each point of intersection lying to the right of the point

$$h = \varkappa c_1^2 + \frac{a}{\varkappa} - \frac{\sqrt{a^2 - 4\varkappa b^2}}{\varkappa}$$

(that is, to the right of the point of intersection of the parabola (11) and the line  $k = 0$ ), there are exactly two critical points of rank 0 and the types of these two points coincide. The preimages of all other points of intersection are empty. In other words,

- if  $0 < b^2 < \varkappa^3 c_1^4$  and  $a < f_t(b)$ , where the function  $f_t(b)$  is given by the formula (15), then there is no critical points of rank 0 from this series in the preimage;
- if  $a > f_t(b)$  and  $a > f_k(b)$ , where  $f_k(b)$  is given by the formula (12), then there are 2 point from this series on the orbit;
- if  $f_k(b) > a > f_t(b)$  (it is possible only if  $b^2 > \varkappa^3 c_1^4$ ), then the preimage contains 6 points from this series.
- if  $b^2 > \varkappa^3 c_1^4$  and  $a < f_t(b)$ , then the preimage contains 4 points from this series.

The points corresponding to the points of intersection with the parameter  $z > z_{cusp} = \sqrt[3]{b^2 c_1^2}$ , that is with the parameter greater than the parameter of the cusp of the curve (9) (that is the points  $y_{10}$  and  $z_1$  in Fig. 3–18), have center-center type. If  $a \neq f_t(b)$ , then the points corresponding to the points of intersection with the parameter  $z < z_{cusp} = \sqrt[3]{b^2 c_1^2}$  (that is the point  $y_{11}$  in Fig. 6–8) have center-saddle type.

The proof of Lemma 2 is given in Section 4.3.

As it turned out, in the case under consideration the obtained information about the types of critical points allows us not only to construct the bifurcation diagrams of the momentum mapping but also to determine the types of bifurcations of Liouville tori and the loop molecules for singular points of the momentum mapping. Just as the proof of Theorem 1, the proofs of Theorems 2 and 3 are given in Section 4.4.

Just as in the classical Kovalevskaya case there are only four types of bifurcation of tori corresponding to the smooth regular arcs of the bifurcation diagram. In the terminology from [4] they correspond to the atoms  $A$ ,  $A^*$ ,  $B$  and  $C_2$ .

**THEOREM 2.** *In Fig. 3–30 for each bifurcation diagram of the momentum mapping the bifurcations of Liouville tori corresponding to different arcs of the bifurcation diagrams are specified and all singular points of the bifurcation diagrams are marked.*

The singular points of the bifurcation diagrams are denoted by  $y_1$ – $y_{13}$  and  $z_1$ – $z_{11}$ . These points correspond to the cusps, the points of intersection and tangency of the bifurcation curves that form the bifurcation diagram of the momentum mapping (recall that these curves are described in Lemma 1).

The singular points  $y_1, y_3, y_7, y_{10}$ – $y_{12}$ ,  $z_1, z_3$ – $z_7$  and  $z_9$ – $z_{11}$  correspond to nondegenerate singularities of the momentum mapping  $\mathcal{F} = (H, K) : M_{a,b}^4 \rightarrow \mathbb{R}^2$ . The points marked with the same letters correspond to singularities of the same type. The types of these nondegenerate singularities are given in Lemmas 2 and 4.

The points  $y_2, y_4, y_5, y_6, y_8, y_9, y_{13}$ ,  $z_2$  and  $z_8$  correspond to degenerate one-dimensional orbits of the action of the group  $\mathbb{R}^2$  on  $M_{a,b}$  generated by the Hamiltonian (7) and the integral (8). (In this paper we do not determine the types of critical points of rank 1, but it is possible to make an assumption about their types — most likely they are typical singularities described in [4]. The type of a singularity can be easily guessed from its loop molecule.) The next statement ensures that the singularities in the preimage of all other points of the bifurcation diagrams are nondegenerate.

**ASSERTION 1.** *The considered integrable Hamiltonian systems with Hamiltonian (7) and (8) on all non-singular orbits  $M_{a,b}$  of the Lie algebras  $so(4)$ ,  $e(3)$  and  $so(3, 1)$  are of Bott type. In other words, for all non-singular values of the parameters  $a$  and  $b$  all critical points in the preimage of non-singular points of the bifurcation diagrams (that is, the points that are not cusps or points of intersection or tangency for the smooth arcs of the bifurcation diagrams) are nondegenerate points of rank 1.*

The proof of Assertion 1 is given in Section 4.1. Let us emphasize that in this paper the fact that the systems are of Bott type is proved for all non-singular orbits of the pencil  $so(4) - e(3) - so(3, 1)$ .

**REMARK 6.** It is not hard to understand the structure of the bifurcation diagrams for the remaining non-singular orbits that are not shown in Fig. 3–30. For example in the case  $a = f_k(b)$ ,  $\varkappa > 0$  the parametric curve (9) intersects the line  $k = 0$  at the cusp point. There is no doubt that the critical points of rank 0 at which the structure of bifurcation diagrams changes are degenerate. In section 4.3 during the proof of Lemma 1 we actually prove a more general statement that the remaining points — in a neighbourhood of which the bifurcation diagram does not change its structure when

passing from one area of the plane  $\mathbb{R}^2(a, b)$  to another — remain nondegenerate and their types do not change.

**THEOREM 3.** *The loop molecules for all singular points of the bifurcation diagrams shown in Fig. 3–30 are listed in Tables 2 and 3. The loop molecules for singular points of the diagrams marked with the same letters coincide.*

$y_1$	$A \xrightarrow{r=0} A$	$y_7$	
$y_2$	$A \xrightarrow{r=0} B \xrightarrow{r=0} A$ $A \xrightarrow{r=0} B$		
$y_3$		$y_8$	$A \xrightarrow{r=1/2} B \xrightarrow[r=\infty]{r=\infty} A^*$ twice
		$y_9$	$A \xrightarrow{r=0} B \xrightarrow{r=\infty} A$ twice
$y_4$	$A \xrightarrow{r=0} B \xrightarrow{r=0} A$ $A \xrightarrow{r=0} B$	$y_{10}$	$A \xrightarrow{r=\infty} A$ $A \xrightarrow{r=0} A$ $A \xrightarrow{r=\infty} A$ $A \xrightarrow{r=0} A$
$y_5$	$A \xrightarrow{r=0} C_2 \xrightarrow[r=\infty]{r=\infty} B$		$y_{11}$
		$y_{12}$	$A \xrightarrow{r=\infty} B \xrightarrow{r=\infty} A$ $A \xrightarrow{r=\infty} B$
$y_6$	$A \xrightarrow{r=0} B \xrightarrow{r=\infty} A$	$y_{13}$	$A \xrightarrow{r=0} B \xrightarrow{r=0} A$ twice $A \xrightarrow{r=0} B$

Table 2: Loop molecules, classical Kovalevskaya case.

**REMARK 7.** For the points on the boundary of bifurcation diagrams the loop molecules in Tables 2 and 3 are shown counterclockwise. Although in this case the ambiguity may arise only for the point  $z_2$ . The loop molecule for this point must



three families of curves on the plane  $\mathbb{R}^2(h, k)$ :

1. The line  $k = 0$ ;
2. The union of the parabola

$$k = (h - \varkappa c_1^2)^2 + 4ac_1^2 \quad (17)$$

and the tangent line to this parabola at the point  $h = 0$

$$k = -2\varkappa c_1^2 h + (4ac_1^2 + \varkappa^2 c_1^4); \quad (18)$$

3. The union of two parabolas

$$k = (h - \varkappa c_1^2)^2 \quad (19)$$

and

$$k = \left( h - \varkappa c_1^2 - \frac{2a}{\varkappa} \right)^2. \quad (20)$$

Now in order to construct the bifurcation diagrams of the momentum mapping it remains to throw away several parts of the curves described in Lemma 3. A precise description of the bifurcation diagrams is given in Theorem 4 (see also Fig. 22–25).

Let us now describe the set of critical points of rank 0. The following lemma is proved in Section 4.3, as well as Lemma 2.

LEMMA 4. *Let  $\varkappa > 0$  and  $b = 0$ . Then the image of critical points of rank 0 is contained in the union of the following three families of points:*

1. The point of intersection of the parabolas (19) and (20) (the point  $z_5$  in Fig. 22). This point has coordinates

$$h = \varkappa c_1^2 + \frac{a}{\varkappa}, \quad k = \frac{a^2}{\varkappa^2}.$$

*If  $a > \varkappa^2 c_1^2$ , then there are two critical points of rank 0 in the preimage of the point on the orbit  $M_{a,0}$ . If  $a = \varkappa^2 c_1^2$ , then there is one critical point of rank 0 in the preimage, and if  $a < \varkappa^2 c_1^2$ , then there is no critical points of rank 0 in the preimage. If  $a > \varkappa^2 c_1^2$  then all critical points from this series are nondegenerate critical points of saddle-center type.*

2. The point of intersection of the upper parabola (17) and the tangent line (18) with the parabolas (19) and (20).

*For any  $a > 0$  there are two points of intersection of the line (18) and the left parabola (19) with coordinates*

$$h = \pm 2\sqrt{ac_1}, \quad k = (\pm 2\sqrt{ac_1} - \varkappa^2 c_1^2)^2$$

*and there is exactly one critical point of rank 0 in the preimage of each of these points on the orbit  $M_{a,0}$ .*

- (a) The critical point in the preimage of the upper point of intersection (that is the point  $y_1$  in Fig. 22 - 25) is a nondegenerate critical point of center-center type.
- (b) If  $a > \varkappa^2 c_1^2$ , then the critical point  $p$  in the preimage of the lower point of intersection (that is the point  $y_3$  in Fig. 22,  $z_{10}$  in Fig. 23 and  $z_9$  in Fig. 24, 25) is a nondegenerate critical point of saddle-saddle type. If  $\frac{\varkappa^2 c_1^2}{4} < a < \varkappa^2 c_1^2$ , then  $p$  is a nondegenerate critical point of saddle-center type and if  $a < \frac{\varkappa^2 c_1^2}{4}$ , then  $p$  is a nondegenerate critical point of center-center type.
- (c) There are two critical points of rank 0 in the preimage of the intersection point of the upper parabola (17) with the right parabola (20) (the point  $z_7$  in Fig. 22-25)

$$h = \frac{a}{\varkappa}, \quad k = \left(\frac{a}{\varkappa} - \varkappa c_1^2\right)^2 + 4ac_1^2$$

on each orbit  $M_{a,0}$  (where  $a > 0$ ) and both points in the preimage are nondegenerate critical points of center-center type.

3. The point of intersection of the line  $k = 0$  and the tangent line (18) (the point  $z_1$  in Fig. 22 and 23). This point has coordinates

$$h = \frac{\varkappa c_1^2}{2} + \frac{2a}{\varkappa}, \quad k = 0.$$

If  $a > \frac{\varkappa^2 c_1^2}{4}$ , then there are two critical points of rank 0 of center-center type in the preimage of this point on the orbit  $M_{a,0}$ . If  $a = \frac{\varkappa^2 c_1^2}{4}$ , then there is one point critical point of rank 0 in the preimage, and if  $a < \frac{\varkappa^2 c_1^2}{4}$ , then there is no critical points of rank 0 in the preimage.

In the case when  $\varkappa > 0$  and  $b = 0$  there are three qualitatively different types of bifurcation diagrams. This is due to the fact that the functions  $f_k, f_r, f_m, f_t$  and  $f_l$  given by the formulas (12), (13), (14), (15) and (16) respectively divide the ray  $\{b = 0, a \geq 0\}$  into 3 parts.

**THEOREM 4.** *In the case when  $\varkappa > 0$  and  $b = 0$  the form of the bifurcation diagram depends on the parameter  $a$ . In the following three cases the diagrams are qualitatively different:*

1.  $0 < a < \frac{\varkappa^2 c_1^2}{4}$ ,
2.  $\frac{\varkappa^2 c_1^2}{4} < a < \varkappa^2 c_1^2$ ,
3.  $\varkappa^2 c_1^2 < a$ .

The corresponding bifurcation diagrams are shown in Fig. 22-25, where the formulas for the lines and parabolas are given in Lemma 3.

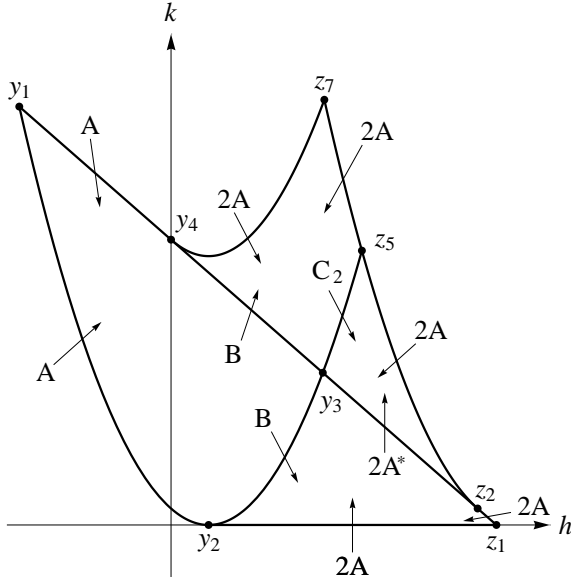


Figure 22: Area X:  $b = 0$ ,  $\varkappa^2 c_1^2 < a$

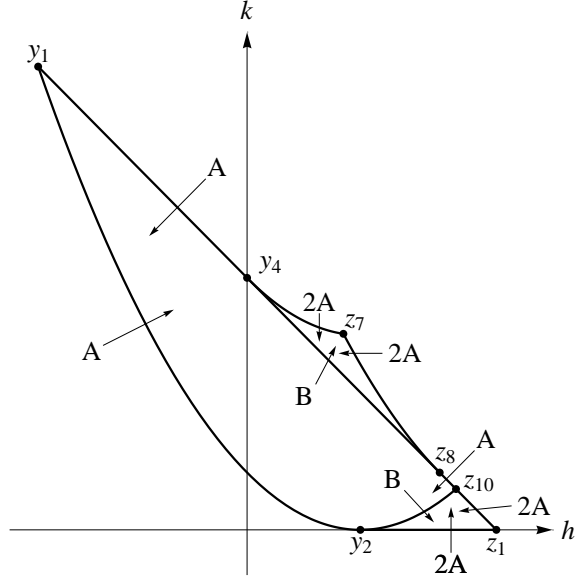


Figure 23: Area XI:  $b = 0$ ,  $\frac{\varkappa^2 c_1^2}{4} < a < \varkappa^2 c_1^2$

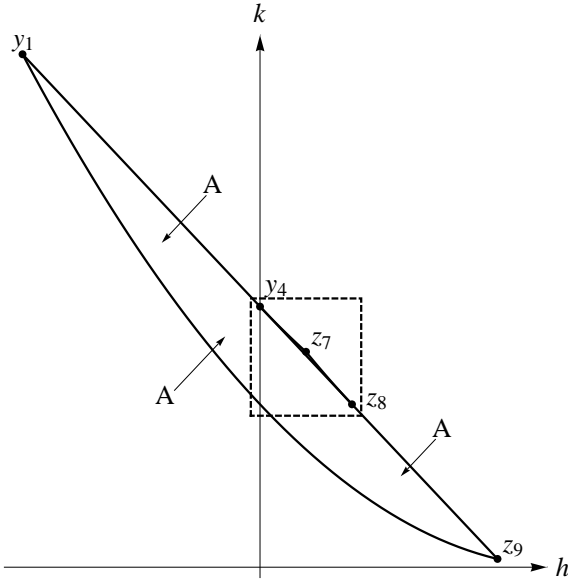


Figure 24: Area XII:  $b = 0$ ,  $0 < a < \frac{\varkappa^2 c_1^2}{4}$

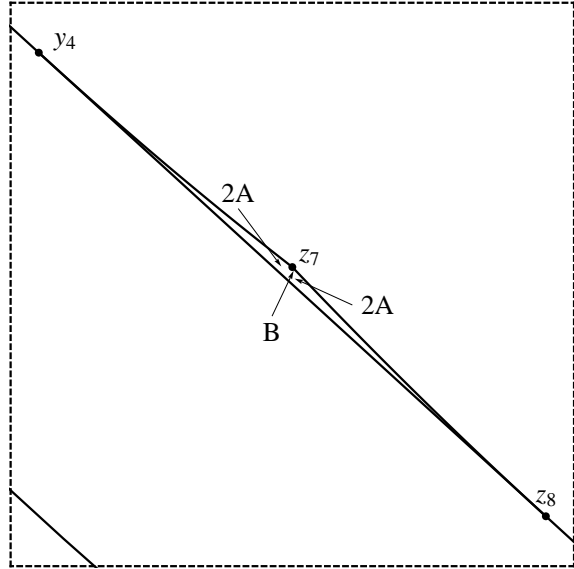


Figure 25: Area XII: an enlarged fragment of Fig. 24

REMARK 9. In Fig. 22–25 the arcs  $z_2 z_1$ ,  $z_8 z_9$  and  $z_8 z_{10}$  belong to the line (18) and the arc  $y_4 z_7$  belongs to the upper parabola (17). The rest of the arcs distribute between the curves in an obvious way.

Bifurcation diagrams for the case  $b = 0$  were also previously described in the paper [14].

The bifurcations of Liouville tori and the loop molecules for the singular points are

described earlier in Theorems 2 and 3 respectively.

## 4 Proof of the main statements

### 4.1 Critical points of rank 1

In this section we prove Lemmas 1 and 3, which claim that the bifurcation diagrams are contained in the curves described in these lemmas. For this we first describe all critical points of the momentum mapping in Assertion 2 and then study their image under the momentum mapping. Note that all these critical points apart from the points from Assertion 15 are critical points of rank 1.

Let us emphasize that in this section we do not impose restrictions on the parameters  $\varkappa$  and  $b$  (that is  $\varkappa, b \in \mathbb{R}$ , unless otherwise stated).

**ASSERTION 2.** *The set of points where the Hamiltonian vector fields corresponding to the Hamiltonian (7) and the integral (8) are linearly dependent is the union of the following six families of points. The first three families are three-parametric and the last three families are four-parametric.*

*Four-parameter families:*

1.  $x_1 = \frac{\varkappa c_1^2 + J_1^2 - J_2^2}{2c_1}, \quad x_2 = \frac{J_1 J_2}{c_1}$
2.  $J_2 = 0, \quad x_3 = \frac{J_1 J_3}{c_1}$
3.  $x_1 = \varkappa c_1 + (J_1 - c_1 \frac{x_3}{J_3}) \frac{x_2}{J_2}, \quad x_2 = J_2 \frac{(J_1 x_3 - \varkappa c_1 J_3)(J_1 J_3 - c_1 x_3) + J_2^2 J_3 x_3}{(J_1 J_3 - c_1 x_3)^2 + J_2^2 J_3^2},$   
where  $J_2 J_3 \neq 0$ .

*Three-parameter families:*

4.  $J_2 = 0, \quad x_2 = 0, \quad J_1 x_3 - J_3 x_1 = 0$
5.  $J_3 = 0, \quad x_3 = 0,$   
 $((x_1 - \varkappa c_1) J_1 + J_2 x_2)(J_2(x_1 - \varkappa c_1) - J_1 x_2) + c_1 x_2(x_1(x_1 - \varkappa c_1) + x_2^2) = 0$
6.  $J_1 = 0, \quad J_3 = 0, \quad x_2 = 0$

*Proof.* The points at which the Hamiltonian vector fields  $X_H$  and  $X_K$  are linearly dependent are exactly the points at which all 15 rank 2 minors of the matrix  $(X_H, X_K)$  composed from the coordinates of the vectors  $X_H$  and  $X_K$  are equal to zero.

Note that the minor  $\Delta_{13}$  corresponding to the first and the third lines has form

$$\begin{vmatrix} \{J_1, H\} & \{J_1, K\} \\ \{J_3, H\} & \{J_3, K\} \end{vmatrix} = 16c_1(c_1 x_2 - J_1 J_2)(J_2 J_3(\varkappa c_1 - x_1) + (J_1 J_3 - c_1 x_3)x_2)$$

Therefore either  $x_2 = \frac{J_1 J_2}{c_1}$  or  $J_2 J_3(\varkappa c_1 - x_1) + (J_1 J_3 - c_1 x_3)x_2 = 0$ .

First, we examine the case  $x_2 = \frac{J_1 J_2}{c_1}$ . Substituting  $x_2$  in the matrix consisting of minors we immediately obtain the first solution

$$x_1 = \frac{\varkappa c_1^2 + J_1^2 - J_2^2}{2c_1}, \quad x_2 = \frac{J_1 J_2}{c_1}. \quad (21)$$

The rest of the proof is by exhaustion. If  $x_3 = \frac{J_1 J_3}{c_1}$ , then we obtain the following three families of solutions:

$$x_1 = \varkappa c_1, \quad x_2 = \frac{J_1 J_2}{c_1}, \quad x_3 = \frac{J_1 J_3}{c_1}, \quad (22)$$

$$J_2 = 0, \quad x_2 = 0, \quad x_3 = \frac{J_1 J_3}{c_1}, \quad (23)$$

$$J_1 = 0, \quad J_3 = 0, \quad x_2 = 0, \quad x_3 = 0. \quad (24)$$

If  $x_3 \neq \frac{J_1 J_3}{c_1}$ , then we get the following two families of solutions:

$$J_1 x_3 - J_3 x_1 = 0, \quad J_2 = 0, \quad x_2 = 0, \quad (25)$$

$$J_1 = 0, \quad J_3 = 0, \quad x_2 = 0. \quad (26)$$

Now suppose that  $J_2 J_3 (\varkappa c_1 - x_1) + (J_1 J_3 - c_1 x_3) x_2 = 0$ ,  $x_2 \neq \frac{J_1 J_2}{c_1}$ . There are two variants: either  $J_2 J_3 = 0$  or  $x_1 = \frac{\varkappa c_1 J_2 J_3 + J_1 J_3 x_2 - c_1 x_2 x_3}{J_2 J_3}$ .

If  $J_2 = 0$ , then we get the second four-parameter family of points of rank one:

$$J_2 = 0, \quad x_3 = \frac{J_1 J_3}{c_1}. \quad (27)$$

And if  $J_2 \neq 0$ ,  $J_3 = 0$ , then we obtain the following solution:

$$\begin{aligned} J_3 = 0, \quad x_3 = 0, \\ ((x_1 - \varkappa c_1) J_1 + J_2 x_2) (J_2 (x_1 - \varkappa c_1) - J_1 x_2) + c_1 x_2 (x_1 (x_1 - \varkappa c_1) + x_2^2) = 0. \end{aligned} \quad (28)$$

Not let us consider the case  $x_1 = \frac{\varkappa c_1 J_2 J_3 + J_1 J_3 x_2 - c_1 x_2 x_3}{J_2 J_3}$ . It is easy to check that in this case the minor  $\Delta_{12}$  is equal to

$$-16c_1 (x_2 (J_2^2 J_3^2 + (J_1 J_3 - c_1 x_3)^2) - J_2 ((\varkappa c_1^2 + J_1^2 + J_2^2) J_3 x_3 - c_1 J_1 x_3^2 - \varkappa c_1 J_1 J_3^2)).$$

The coefficient by  $x_2$  is not equal to zero since the case  $J_2 J_3 = 0$  has already been analyzed. Expressing  $x_2$  from this equation we obtain the ninth solution:

$$\begin{aligned} x_1 &= \frac{\varkappa c_1 J_2 J_3 + J_1 J_3 x_2 - c_1 x_2 x_3}{J_2 J_3}, \\ x_2 &= J_2 \frac{(\varkappa c_1^2 + J_1^2 + J_2^2) J_3 x_3 - c_1 J_1 x_3^2 - \varkappa c_1 J_1 J_3^2}{(J_1 J_3 - c_1 x_3)^2 + J_2^2 J_3^2}. \end{aligned} \quad (29)$$

Thus we have considered all the cases. It remains to collect all the solutions together. It is obvious that the family (24) is a particular case of the solution (26) and that the solution (23) is a special case of the solution (27). It remains to note that the family (22) is contained in the families (27), (28) and (29). Assertion 2 is proved.  $\square$

Now let us prove Lemma 1. For this, we show that the images of the critical points from Assertion 2 belong to the curves described in Lemma 1.

ASSERTION 3. *Let  $\varkappa \neq 0$  and  $b \neq 0$ . Then the images of the families of critical points described in Assertion 2 are arranged as follows:*

1. *The images of critical points from the family 1 lie on the line  $k = 0$ .*
2. *The images of critical points from the family 2 belong to the curve (9).*
3. *The images of critical points from the families 3, 4, 5 and 6 lie on the union of two parabolas (10) and (11).*

*Proof.* 1. It is explicitly checked that  $k = 0$ .

2. The equation (9) can be obtained as follows. Take the function  $J_3^2 + c_1 x_1$  as the parameter  $z$ . Note that  $J_3^2 + c_1 x_1 \neq 0$  since  $b \neq 0$ . Therefore,  $J_1$  can be expressed from the formula for  $b$  and then  $x_2$  can be expressed from the formula for  $a$ . It remains to substitute the obtained expressions for  $J_1$  and  $x_2$  in the equations for the Hamiltonian (7) and the first integral (8) and then replace  $J_3^2 + c_1 x_1$  by  $z$ . As a result, the equations (7) and (8) take the form (9), as required.
3. It can be explicitly checked that for any point from the Families 3, 4 and 5 one of the two equations (10) and (11) holds.

In this case it is easier to verify first that  $k = \left(-\frac{\lambda}{2}\right)^2$ , where  $\lambda$  is the coefficient of proportionality between  $X_K$  and  $X_H$  (that is  $X_K + \lambda X_H = 0$ ), and then to check that

$$-\frac{\lambda}{2} = h - \varkappa c_1^2 - \frac{a}{\varkappa} \pm \frac{\sqrt{a^2 - 4\varkappa b^2}}{\varkappa}.$$

While testing this equality it is convenient to use the relation

$$\frac{a}{b} = \frac{x_3}{J_3} + \varkappa \frac{J_3}{x_3},$$

which holds if  $J_3 \neq 0$  and  $x_3 \neq 0$ .

Assertion 3 is proved. □

In what follows we need the following statement about the critical points of the family 2 from Assertion 2.

ASSERTION 4. *Let  $\varkappa \neq 0$  and  $b \neq 0$ . Then for  $z^2 > \frac{a + \sqrt{a^2 - 4\varkappa b^2}}{2} c_1^2$  either there is no critical points in the preimage of points of the curve (9) or the critical points in the preimage from two critical circles and the symmetry  $(J_3, x_3) \rightarrow (-J_3, -x_3)$  interchanges these circles.*

*Proof.* It is not hard to check that for a fixed parameter  $z$  the critical points from the family 2 are given by the following equations

$$J_1 = \frac{bc_1}{z}, \quad J_2 = 0, \quad x_1 = \frac{z - J_3^2}{c_1}, \quad x_3 = \frac{b}{z} J_3,$$

where the coordinates  $J_3$  and  $x_2$  satisfy an equation of the form

$$\left(\frac{J_3^2}{c_1} + d\right)^2 + x_2^2 = R^2 \quad (30)$$

for some constants  $d$  and  $R$  depending on  $\varkappa, a, b$  and  $z$ . Thus in order to prove the assertion it remains to prove that  $J_3 \neq 0$  for  $z^2 > \frac{a + \sqrt{a^2 - 4\varkappa b^2}}{2} c_1^2$ . It is not hard to verify explicitly: if  $J_3 = 0$ , then the equation (30) has the form

$$z^4 - ac_1^2 z^2 + \varkappa b^2 c_1^4 = 0,$$

which has a solution precisely when

$$\frac{a - \sqrt{a^2 - 4\varkappa b^2}}{2} c_1^2 < z^2 < \frac{a + \sqrt{a^2 - 4\varkappa b^2}}{2} c_1^2.$$

Assertion 4 is proved. □

Now let us prove Lemma 3.

ASSERTION 5. *Let  $\varkappa \neq 0$  and  $b = 0$ . Then the images of the families of critical points described in Assertion 2 are arranged as follows:*

1. *The images of critical points from the family 1 lie on the line  $k = 0$ .*
2. *The images of critical points from the family 2 belong to the union of the parabola (17) and the tangent line (18).*
3. *Images of the critical points from the families 3, 4, 5 and 6 lie on the union of two parabolas (19) and (20).*

*Proof.* The proof of this statement is almost identical to the proof of Assertion 3 except for the following. First, the case  $J_3^2 + c_1 x_1 = 0$  should be considered while determining the image of the family 2. It is not hard to check explicitly that in this case the image lies on the parabola (17). Second, we have to consider the family 6 and show that its image lies on the left parabola (19). □

We now prove Assertion 1 about the nondegeneracy of critical points of rank 1. In order to prove it we use the following simple criterion of nondegeneracy for critical points of rank 1 (see [4]).

ASSERTION 6. *Let  $(M^4, \omega)$  be a symplectic manifold and  $y_0 \in (M, \omega)$  be a critical point of rank 1 for an integrable system with Hamiltonian  $H$  and integral  $K$ . Denote by  $F = \alpha H + \beta K$  a nontrivial linear combination for which the point  $y_0$  is a critical point and by  $A_F$  the linearization of the corresponding Hamiltonian vector field  $X_F$  at this point  $y_0$ . The point  $y_0$  is nondegenerate if and only if the operator  $A_F$  has a non-zero eigenvalue.*

In the case under consideration the system is defined on a Poisson manifold. Hence it is convenient to use the following statement.

ASSERTION 7. Suppose that in local coordinates  $(p^1, \dots, p^k, q^1, \dots, q^k, z^1, \dots, z^m)$  in a neighbourhood of a point  $x_0$  a Poisson bracket has the form  $\sum_{i=1}^k \frac{\partial}{\partial p^i} \wedge \frac{\partial}{\partial q^i}$ . Suppose also that  $x_0$  is a critical point for a Hamiltonian vector field  $X_F$  with Hamiltonian  $F$ . Then the linearization  $A_F$  of the Hamiltonian vector field  $X_F$  has the form

$$\begin{aligned} & \left( \frac{\partial^2 F}{\partial q^i \partial p^j} \frac{\partial}{\partial p^i} \otimes dp^j + \frac{\partial^2 F}{\partial q^i \partial q^j} \frac{\partial}{\partial p^i} \otimes dq^j + \frac{\partial^2 F}{\partial q^i \partial z^j} \frac{\partial}{\partial p^i} \otimes dz^j \right) - \\ & \left( \frac{\partial^2 F}{\partial p^i \partial p^j} \frac{\partial}{\partial q^i} \otimes dp^j + \frac{\partial^2 F}{\partial p^i \partial q^j} \frac{\partial}{\partial q^i} \otimes dq^j + \frac{\partial^2 F}{\partial p^i \partial z^j} \frac{\partial}{\partial q^i} \otimes dz^j \right). \end{aligned}$$

Thus if  $\hat{F}$  is the restriction of the function  $F$  to a symplectic leaf, then the spectrum of the linearization of the vector field  $X_F$  can be obtained from the spectrum of the linearization of the vector field  $X_{\hat{F}}$  by adding zeros in the amount equal to the codimension of the symplectic leaf. Therefore, as well as in the symplectic case, in order to check the nondegeneracy of points of rank 1 it is sufficient to verify that the spectrum of the corresponding operator does not consist solely of zeros.

This can be verified explicitly. To simplify the verification in the following assertion we specify the coefficient of proportionality  $\lambda$  between the Hamiltonian vector fields corresponding to the Hamiltonian (7) and the integral (8) as well as describe the spectrum of the linearization of the corresponding Hamiltonian vector field  $X_{K+\lambda H}$  for all critical points of rank 1 of the integrable Hamiltonian system under consideration (that is, for all points from Assertion 2 except for the points of rank 0 from Assertion 15).

ASSERTION 8. For each critical point of rank 1 from Assertion 2 we specify  $\lambda$  such that  $X_K + \lambda X_H = 0$  at this point and  $\mu$  such that the spectrum of the operator  $A_{K+\lambda H}$  consists of four zero and  $\pm\mu$ .

Four-parameter families:

1. Family 1. The coefficient of proportionality  $\lambda = 0$ , that is  $X_K = (0, 0, 0, 0, 0, 0)$ .  
The nontrivial eigenvalue:

$$\mu = 8i |(\varkappa c_1^2 + J_1^2 + J_2^2) J_3 - 2c_1 J_1 x_3|.$$

2. Family 2. The coefficient of proportionality:

$$\lambda = 2(\varkappa c_1^2 - J_1^2),$$

the square of the eigenvalue:

$$\mu^2 = 64c_1 (J_1^2 - J_3^2 - c_1 x_1) ((J_1^2 - c_1 x_1) (x_1 - \varkappa c_1) - c_1 x_2^2).$$

3. Family 3. The coefficient of proportionality:

$$\lambda = 2 \left( \varkappa c_1^2 + J_1^2 + J_2^2 - 2c_1 J_1 \frac{x_3}{J_3} \right),$$

the square of the eigenvalue:

$$\mu^2 = -32\lambda \left( (J_1 J_3 - c_1 x_3)^2 + \left( (J_1^2 + J_2^2) - c_1 \frac{J_1 x_3}{J_3} \right)^2 + J_2^2 (\varkappa c_1^2 + J_3^2) \right).$$

Three-parameter families:

4. Family 4. The coefficient of proportionality:

$$\lambda = 2 (\varkappa c_1^2 + J_1^2 - 2c_1 x_1),$$

the square of the eigenvalue:

$$\mu^2 = -32\lambda ((J_1^2 - c_1 x_1)^2 + (J_1 J_3 - c_1 x_3)^2)$$

5. Family 5. In this item we assume that  $x_2 \neq 0$  since all point from the family 5 that satisfy the condition  $x_2 = 0$  either have rank 0 or belong to the family 6. The coefficient of proportionality:

$$\lambda = 2(\varkappa c_1^2 - J_1^2 + J_2^2) + \frac{4}{x_2} J_1 J_2 (x_1 - \varkappa c_1).$$

If in addition  $x_1 \neq \frac{\varkappa c_1^2 + J_1^2 - J_2^2}{2c_1}$ , then the square of the eigenvalue is equal to:

$$\mu^2 = \frac{16\lambda^2 J_2 \gamma}{x_2 (\varkappa c_1^2 + J_1^2 - J_2^2 - 2c_1 x_1)},$$

where

$$\gamma = (c_1 J_1 x_2^2 - J_1 (x_1 - \varkappa c_1) (J_1^2 - J_2^2 - c_1 x_1) - J_2 x_2 (\varkappa c_1^2 + J_1^2 - J_2^2 - 2c_1 x_1)).$$

If  $x_1 = \frac{\varkappa c_1^2 + J_1^2 - J_2^2}{2c_1}$ , then either  $x_2 = \frac{J_1 J_2}{c_1}$  or  $x_2 = \pm \frac{\varkappa c_1^2 - J_1^2 + J_2^2}{2c_1}$ . In the first case  $\mu = 0$ , in the second case

$$\mu^2 = -32J_2^2 \lambda (\varkappa c_1^2 + (J_1 \mp J_2)^2).$$

6. Family 6. The coefficient of proportionality:

$$\lambda = 2 (\varkappa c_1^2 - J_2^2 - 2c_1 x_1),$$

the square of the eigenvalue:

$$\mu^2 = -32\lambda c_1^2 (\varkappa J_2^2 + x_1^2 + x_3^2).$$

*Assertion 1.* We use Assertion 6 to prove the nondegeneracy of points of rank 1. The coefficients of proportionality and the spectrum of the corresponding operators are described in Assertion 8. After that the nondegeneracy is proved by exhaustion. Assertion 1 is proved.  $\square$

## 4.2 Types of bifurcation diagrams. (Case $b \neq 0$ )

In this section we show that the curves from Lemma 1 are positioned relative to each other as it is shown in Fig. 3–21 (for the corresponding values of the parameters  $a$  and  $b$ ). Thereby we actually describe all possible bifurcation diagrams of the momentum mapping. We are interested in the singular points of bifurcation diagrams, that is in the cusps, in the points of intersection and tangency of these curves in the first place.

First of all, it is obvious that for any values of the parameters  $a$  and  $b$  the parabolas (10) and (11) intersect the line  $k = 0$  at the points

$$h = \varkappa c_1^2 + \frac{a}{\varkappa} - \frac{\sqrt{a^2 - 4\varkappa b^2}}{\varkappa}, \quad \text{and} \quad h = \varkappa c_1^2 + \frac{a}{\varkappa} + \frac{\sqrt{a^2 - 4\varkappa b^2}}{\varkappa}$$

respectively and intersect each other at the point

$$h = \varkappa c_1^2 + \frac{a}{\varkappa}, \quad k = \frac{a^2 - 4\varkappa b^2}{\varkappa^2}. \quad (31)$$

Thus, it remains to describe the relative position of the curve (9) with respect to the line  $k = 0$  and the parabolas (10), (11).

In this section we first describe this curve (9) (see Assertion 9), then we determine the number of its points of intersection with the parabolas described above (see Assertion 10) and the line  $k = 0$  (see Assertion 11). After that the rest of the section is devoted to the study of the mutual interposition of the found “singular” points. The final result can be formulated as.

LEMMA 5. *The functions  $f_k, f_r, f_m, f_t$  and  $f_l$  given by the formulas (12), (13), (14), (15) and (16) respectively divide the area  $\{b > 0, a > 2\sqrt{\varkappa b}\}$  into 9 sub-areas. For each of these sub-areas the cusps, the point of intersection and tangency of the line  $k = 0$ , the parabolas (10), (11) and the curve (9) are located on this four curves as it is shown in Fig. 3–21.*

We begin with a description of the curve (9).

ASSERTION 9. *Let  $\varkappa \neq 0$ . Then for any  $a, b \in \mathbb{R}, b \neq 0$ , the curve (9) has one cusp point*

$$z_{cusp} = \sqrt[3]{b^2 c_1^2} \quad (32)$$

*and two points of local extrema*

$$z_{+ext} = \frac{|b|}{\sqrt{\varkappa}} \quad \text{and} \quad z_{-ext} = -\frac{|b|}{\sqrt{\varkappa}}. \quad (33)$$

*The point  $z_{-ext}$  is a local minimum for any values of the parameters  $a$  and  $b$ . If  $b > \varkappa^{3/2} c_1^2$ , then the point  $z_{+ext}$  is a local maximum. If  $b < \varkappa^{3/2} c_1^2$ , then the point  $z_{+ext}$  is a local minimum. (If  $b = \varkappa^{3/2} c_1^2$ , then the point  $z_{+ext}$  coincides with the cusp  $z_{cusp}$ .) In other words, the function  $k(z)$  monotonically increases between the points  $z_{+ext}$  and  $z_{cusp}$  and monotonically decreases on the remaining parts of the ray  $z > 0$ .*

*The graph of the corresponding function is convex upward for  $z < z_{cusp}$  and convex downward for  $z > z_{cusp}$ .*

As  $z \rightarrow \pm\infty$  the curve (9) asymptotically tends to the line

$$k = -2\kappa c_1^2 h + (4ac_1^2 \kappa^2 c_1^4).$$

Moreover, as  $z \rightarrow \pm 0$  both functions  $h(z)$  and  $k(z)$  simultaneously tend to  $+\infty$  and besides

$$\frac{k(z)}{h^2(z)} \xrightarrow{z \rightarrow \pm 0} 1.$$

We now describe the points of intersection of the curve (9) with the other curves: with the parabolas (10) and (11) and the line  $k = 0$ . We start with the points of intersection with the parabolas. The proof of the following assertion is by direct computation.

ASSERTION 10. *Let  $\kappa \neq 0$  and  $b \neq 0$ . Then the curve (9) and the left parabola (10) have two points of intersection and one point of tangency. For the points of intersection the corresponding values of the parameter  $z_{+l}$  and  $z_{-l}$  are given by the relation*

$$z^2 = \frac{a + \sqrt{a^2 - 4\kappa b^2}}{2} c_1^2. \quad (34)$$

The tangency point corresponds to the value of the parameter

$$z_{lt} = \frac{a - \sqrt{a^2 - 4\kappa b^2}}{2\kappa}. \quad (35)$$

Analogously, the curve (9) and the right parabola (11) have two points of intersection with the corresponding values of the parameter  $z_{+r}$  and  $z_{-r}$  given by the relation

$$z^2 = \frac{a - \sqrt{a^2 - 4\kappa b^2}}{2} c_1^2 \quad (36)$$

and one point of tangency corresponding to the value of the parameter

$$z_{rt} = \frac{a + \sqrt{a^2 - 4\kappa b^2}}{2\kappa}. \quad (37)$$

REMARK 10. In Assertion 10 (and further in the text) we assume that  $z_{+l} > 0$  and  $z_{+r} > 0$ . As a consequence  $z_{-l} < 0$  and  $z_{-r} < 0$ .

Now let us find the number of intersection points of the line  $k = 0$  and the curve (9).

ASSERTION 11. *Suppose that  $\kappa > 0$ . Then the number of intersection points of the line  $k = 0$  and the curve (9) depends on the values of the parameters  $a$  and  $b$  as follows. Consider the function*

$$f_k(b) = \frac{3b^{4/3} + 6\kappa b^{2/3} c_1^{4/3} - \kappa^2 c_1^{8/3}}{4c_1^{2/3}}.$$

1. Assume that  $b > \kappa^{3/2} c_1^2$ . If  $a > f_k(b)$ , then the line  $k = 0$  and the curve (9) have exactly 3 points of intersection. If  $a < f_k(b)$ , then there is only 1 point of intersection and if  $a = f_k(b)$ , then there are 2 points of intersection.

2. Assume that  $0 < b < \varkappa^{3/2}c_1^2$ . If  $a < f_k(b)$ , then the line  $k = 0$  and the curve (9) have exactly 3 points of intersection. If  $a > f_k(b)$ , then there is only 1 point of intersection and if  $a = f_k(b)$ , then there are 2 points of intersection.
3. If  $b = \varkappa^{3/2}c_1^2$ , then the line  $k = 0$  and the curve (9) have exactly 1 point of intersection for any value of the parameter  $a$ .

The results of Assertion 11 are collected together in table 4.

	$0 < b^2 < \varkappa^3 c_1^4$	$b^2 = \varkappa^3 c_1^4$	$b^2 > \varkappa^3 c_1^4$
$a > f_k(b)$	1	1	3
$a = f_k(b)$	2	1	2
$a < f_k(b)$	3	1	1

Table 4: Number of intersection points of the curve (9) and the line  $k = 0$ .

*Proof.* It is clear that there is no points of intersection if  $z < 0$  since

$$k(z) = 4ac_1^2 - 4\varkappa c_1^2 z - \frac{4b^2 c_1^2}{z} + \left( \frac{b^2 c_1^2}{z^2} - \varkappa c_1^2 \right)^2 > 0.$$

It follows from Assertion 9 that the function  $k(z)$  has two local extrema if  $z > 0$ :

$$z_{+\text{ext}} = \frac{b}{\sqrt{\varkappa}} \quad \text{and} \quad z_{\text{cusp}} = \sqrt[3]{b^2 c_1^2}.$$

It remains to examine the location of these extrema and whether the value of the function  $k(z)$  at these points is greater than zero. Assertion 11 is proved.  $\square$

Thus we found the points  $z_{\text{cusp}}, z_{\pm\text{ext}}, z_{\pm l}, z_{\pm r}, z_{lt}$  and  $z_{rt}$  on the curve (9) given by the formulas (32), (33), (34), (35), (36) and (37) respectively. We now determine the order of these points on the  $z$ -axis. It is obvious that

$$z_{-l} < z_{-\text{ext}} < z_{-r} < 0,$$

and that the value of the parameter  $z$  for the other described points is greater than zero. The next assertion is proved by direct calculation.

**ASSERTION 12.** *Let  $\varkappa > 0$ . Then, depending on the values of the parameters  $a$  and  $b$ , the points  $z_{\text{cusp}}, z_{+\text{ext}}, z_{+l}, z_{+r}, z_{lt}$  and  $z_{rt}$  (described in Assertions 9 and 10) are arranged on the ray  $z > 0$  so as it is described in Tables 5 and 6. Here functions  $f_r(b)$  and  $f_m(b)$  are given by the formulas (13) and (14) respectively.*

We now describe when three curves intersect at one point.

**ASSERTION 13.** *Suppose that  $\varkappa > 0$ ,  $b \neq 0$  and  $a^2 - 4\varkappa b^2 > 0$ . Then the line  $k = 0$ , the curve (9) and the right parabola (11) can not intersect at one point. The line  $k = 0$ , the curve (9) and the left parabola (10) intersect at one point if and only if*

$$a = \left( \frac{\varkappa c_1^2 + t^2}{2c_1} \right)^2 + \varkappa t^2, \quad b = t \left( \frac{\varkappa c_1^2 + t^2}{2c_1} \right) \quad (38)$$

for some  $t \in \mathbb{R}$ .

$a > f_m(b)$	$z_{rt} > z_{+l} > z_{\text{cusp}} > z_{+\text{ext}} > z_{+r} > z_{lt}$
$a = f_m(b)$	$z_{rt} = z_{+l} > z_{\text{cusp}} > z_{+\text{ext}} = z_{+r} > z_{lt}$
$f_r(b) < a < f_m(b)$	$z_{+l} > z_{rt} > z_{\text{cusp}} > z_{+r} > z_{+\text{ext}} > z_{lt}$
$a = f_r(b)$	$z_{+l} > z_{rt} = z_{\text{cusp}} = z_{+r} > z_{+\text{ext}} > z_{lt}$
$a < f_r(b)$	$z_{+l} > z_{+r} > z_{\text{cusp}} > z_{rt} > z_{+\text{ext}} > z_{lt}$

Table 5: Interposition of points of the curve (9) for  $0 < b^2 < \varkappa^3 c_1^4$ .

$a > f_m(b)$	$z_{rt} > z_{+l} > z_{+\text{ext}} > z_{\text{cusp}} > z_{+r} > z_{lt}$
$a = f_m(b)$	$z_{rt} > z_{+l} = z_{+\text{ext}} > z_{\text{cusp}} > z_{+r} = z_{lt}$
$f_r(b) < a < f_m(b)$	$z_{rt} > z_{+\text{ext}} > z_{+l} > z_{\text{cusp}} > z_{lt} > z_{+r}$
$a = f_r(b)$	$z_{rt} > z_{+\text{ext}} > z_{+l} = z_{\text{cusp}} = z_{lt} > z_{+r}$
$a < f_r(b)$	$z_{rt} > z_{+\text{ext}} > z_{lt} > z_{\text{cusp}} > z_{+l} > z_{+r}$

Table 6: Interposition of points of the curve (9) for  $b^2 > \varkappa^3 c_1^4$ .

Note that in the formula (38) the parameter  $a$  is uniquely determined by  $b$ , therefore the formula (38) defines a function, which we denoted by  $a = f_t(b)$  (see the formula (15)).

*of Assertion 13.* It is not hard to check that under the conditions of the assertion the points of rank 1 that belong to the families 1, 2 and also to one of the families 3, 4, 5 and 6 are the points

$$x_1 = \frac{\varkappa c_1^2 + J_1^2}{2c_1}, \quad J_2 = 0, \quad J_3 = 0, \quad x_2 = 0, \quad x_3 = 0.$$

For these points the equality (38) holds with  $t = J_1$ . Therefore, if the equality (38) holds, then the curves intersect at one point.

We now show that if three curves intersect at one point, then the equality (38) holds. It is not hard see that the only point of the curve (9) that can be a point of triple intersection is its point of intersection with the left parabola  $z_{+l}$  (it also easily follows from geometrical considerations). Since by assumption the curves intersect at one point the equality

$$\varkappa c_1^2 + \frac{a}{\varkappa} - \frac{\sqrt{a^2 - 4\varkappa b^2}}{\varkappa} = \frac{b^2 c_1^2}{z_{+l}^2} + 2z_{+l}$$

holds. Substituting the equality (34) we get

$$(z - \varkappa c_1^2)^2 = \sqrt{a^2 - 4\varkappa b^2} c_1^2. \quad (39)$$

If we put

$$z = \frac{t^2 + \varkappa c_1^2}{2},$$

where  $\text{sgn}(t) = \text{sgn}(b)$ , then we get

$$\sqrt{a^2 - 4\varkappa b^2} = \frac{(t^2 - \varkappa c_1^2)^2}{4c_1^2}. \quad (40)$$

Substituting (39) and (40) in the formula (34) we obtain the required expression for  $a$  from the formula (38). This immediately implies the formula (38) for  $b$ . Assertion 13 is proved.  $\square$

It follows from Assertion 9, 10, 11, 12 and 13 that the interposition of the curves from Lemma 1 qualitatively differs depending on position of the parameters  $a$  and  $b$  with respect to the functions  $f_k, f_r, f_m$ , and  $f_t$ , given by the formulas (12), (13), (14) and (15) respectively.

Since in the case  $\varkappa > 0$  the values of the parameters  $a$  and  $b$  always satisfy the inequality  $a^2 - 4\varkappa b^2 \geq 0$  we also consider the function

$$f_l(b) = 2\sqrt{\varkappa}|b|.$$

We now describe how the graphs of the functions  $f_k, f_r, f_m, f_t$  and  $f_l$  are positioned relative to each other. The next assertion is proved by direct calculation.

ASSERTION 14. *Let  $\varkappa > 0$ . Denote by  $\alpha_0$  the only root of the equation  $x^3 + x^2 + x - 1 = 0$ . The graphs of functions  $f_k, f_r, f_m, f_t$  and  $f_l$  given by the formulas (12), (13), (14), (15) and (16) respectively are symmetrical about the axis  $b = 0$  and in the case  $b > 0$  they are positioned as it is shown in Fig. 1 and 2. In other words, for  $b > 0$  all the graphs intersect at the point*

$$M = (\varkappa^{3/2}c_1^2, 2\varkappa^2c_1^2),$$

and the graphs of functions  $f_r$  and  $f_t$  intersect at the point

$$N = (\alpha_0^3\varkappa^{3/2}c_1^2, f_r(\alpha_0^3\varkappa^{3/2}c_1^2)).$$

Further, if  $0 < b^2 < \alpha_0^6\varkappa^3c_1^4$ , then

$$f_k < f_l < f_r < f_t < f_m.$$

If  $\alpha_0^6\varkappa^3c_1^4 < b^2 < \varkappa^3c_1^4$ , then

$$f_k < f_l < f_t < f_r < f_m.$$

And if  $b^2 > \varkappa^3c_1^4$ , then

$$f_l < f_t < f_k < f_r < f_m.$$

of Lemma 5. Lemma 5 easily follows from earlier proved Assertions 9, 10, 11, 12, 13 and simple geometric considerations.  $\square$

### 4.3 Critical points of rank 0

In this section we prove Lemmas 2 and 4 about types of critical points of rank 0. At first we describe all critical points of the momentum mapping of rank 0 and then we find their types and images under the momentum mapping. Recall that on non-singular orbits (that is, on orbits  $M_{a,b}$  such that  $a^2 - 4\varkappa b^2 > 0$ ) non-singular points of rank 0 are precisely the points at which both Hamiltonian vector field  $X_H$  and  $X_K$  vanish. Let us emphasize that the following statement holds for any value of the parameter  $\varkappa \in \mathbb{R}$ .

ASSERTION 15. *The set of points where both Hamiltonian vector fields  $X_H$  and  $X_K$  with Hamiltonians (7) and (8) respectively vanish is the union of the following (two-parameter) families of points in  $\mathbb{R}^6(J, x)$ :*

1.  $(J_1, J_2, 0, \varkappa c_1, 0, 0)$ ,
2.  $(J_1, 0, 0, x_1, 0, 0)$ ,
3.  $(J_1, 0, J_3, \frac{\varkappa c_1^2 + J_1^2}{2c_1}, 0, \frac{J_1 J_3}{c_1})$ .

*Proof.* The vector field  $X_H$  has the following coordinates:

$$\begin{aligned} \{J_1, H\} &= -2J_2J_3, & \{J_2, H\} &= 2J_1J_3 - 2c_1x_3 \\ \{J_3, H\} &= 2c_1x_2, & \{x_1, H\} &= 2J_2x_3 - 4J_3x_2 \\ \{x_2, H\} &= 4J_3x_1 - 2J_1x_3 - 2\varkappa c_1J_3, & \{x_3, H\} &= 2J_1x_2 - 2J_2x_1 + 2\varkappa c_1J_2 \end{aligned}$$

It is easy to see that  $x_2 = 0$  and that either  $J_2 = 0$  or  $J_3 = 0, x_3 = 0$ . The rest of the proof is by exhaustion.  $\square$

of Lemmas 2 and 4. It can be proved by direct calculation that the images of the points of rank 0 lie on these curves. It is possible to explicitly find all the points from the 1 and 2 series on each orbit  $M_{a,b}$ . We now prove the statement about the number of points for the 3 series on the orbit  $M_{a,b}$ . The case  $b = 0$  is trivial, hence we assume that  $b \neq 0$ . It is not hard to verify that the set of points (or rather the corresponding values of the parameters  $J_1$  and  $J_3$ ) is given by the following system of equations

$$\begin{aligned} J_1^5 - 2\varkappa c_1^2 J_1^3 - 4bc_1 J_1^2 + (4ac_1^2 + \varkappa^2 c_1^4) J_1 - 4\varkappa bc_1^3 &= 0 \\ J_3^2 &= \frac{2bc_1 - \varkappa c_1^2 J_1 - J_1^3}{2J_1}. \end{aligned} \tag{41}$$

It is clear that there are exactly two points in the preimage for each point in the image (the coordinates  $J_1$  for these points coincide and the coordinates  $J_3$  are opposite). In order to find the exact number of solutions let us first divide the set of parameters  $(a, b)$  into areas for which this number is constant and then solve this problem for each of the areas. Let us slightly simplify the equation (41) by putting

$$\hat{b} = \frac{b}{\varkappa^{3/2} c_1^2}, \quad \hat{a} = \frac{a}{\varkappa^2 c_1^2}, \quad s = \frac{J_1}{\varkappa^{1/2} c_1}.$$

Then the number of points in the image is equal to the number of solutions of the equation

$$s^5 - 2\hat{b}s^3 - 8\hat{b}s^2 + (4\hat{a} + 1)s - 4\hat{b} = 0 \tag{42}$$

on the segment

$$0 \leq s + s^3 \leq 2\hat{b}. \tag{43}$$

Note that the function  $s + s^3$  is monotonically increasing, so the inequality (43) defines a segment. Note that if we vary the parameters  $a$  and  $b$ , then the number of solutions can change only in the following cases:

1. The equation (42) has multiple roots.
2. One of the endpoints of the segment (43) is a solution of the equation (42). (It is easy to see that the point 0 can not be a root of the equation (42), therefore we only need to check the point  $s + s^3 = 2\hat{b}$ ).

It can be verified that the point  $s + s^3 = 2\hat{b}$  is a solution of the equation (42) if and only if  $a = f_t(b)$  (recall that the function  $f_t(b)$  is defined by the formula (15) and that  $a = f_t(b)$  if and only if three curves of the bifurcation diagram intersect at one point, see Assertion 13). It can also be verified that in a sufficiently small neighbourhood of any point of the curve  $a = f_t(b)$  (except, maybe, for the points at which the equation (42) has multiple roots) the points in the area  $a > f_t(b)$  have one more point in the preimage than the points in the area  $a < f_t(b)$ .

Further, it is easy to verify that the equation (42) has multiple roots in the following cases: either  $a = \pm 2\sqrt{\varkappa}b$  or  $a = f_k(b)$ , where  $f_k(b)$  is given by the formula (12). In the case  $a = 2\sqrt{\varkappa}|b|$  the only multiple root is  $s = 1$  of multiplicity 2. It follows that for  $b^2 < \varkappa^3 c_1^4$  and  $2\sqrt{\varkappa}|b| < a < f_t(b)$  there is no point from the 3 series in the preimage and for  $b^2 > \varkappa^3 c_1^4$  and  $2\sqrt{\varkappa}|b| < a < f_t(b)$  there are exactly two point from the 3 series in the preimage. Since the number of points in the preimage increases by 1 when passing through the curve  $a = f_t(b)$  by increasing the parameter  $a$  (for a fixed  $b$ ) we conclude that in the area  $a > f_t(b), a > f_k(b)$  there is exactly one point in the preimage and there are three points in the preimage for the area  $f_k(b) > a > f_t(b)$ .

Thus the statement about the number of points on each orbit is proved. It remains to prove about the statement about their types. It is not hard to do using the following criteria (for more details see [4]).

**ASSERTION 16.** *Consider a symplectic manifold  $(M^4, \omega)$  and suppose that  $x_0 \in (M, \omega)$  is a critical point of rank 0 for an integrable Hamiltonian system with Hamiltonian  $H$  and integral  $K$ . Then the point  $x_0$  is nondegenerate if and only if the linearizations  $A_H$  and  $A_K$  of the Hamiltonian vector fields  $X_H$  and  $X_K$  at the point  $x_0$  satisfy the following properties:*

1. *the operators  $A_H$  and  $A_K$  are linearly independent,*
2. *there exists a linear combination  $\lambda A_H + \mu A_K$  such that all its eigenvalues are different and not equal to 0.*

*Moreover, if the point  $x_0$  is nondegenerate, then its type is completely determined by the spectrum of any linear combination  $\lambda A_H + \mu A_K$  that has no zero eigenvalues. More precisely the type of the point depends on the type of the spectrum as follows.*

- *If the spectrum of a linear combination  $\lambda A_H + \mu A_K$  has the form  $\alpha, -\alpha, \beta, -\beta$ , where  $\alpha, \beta \in \mathbb{R} - \{0\}$ , then the point  $x_0$  is a critical point of saddle-saddle type.*
- *If the spectrum has the form  $i\alpha, -i\alpha, i\beta, -i\beta$ , where  $\alpha, \beta \in \mathbb{R} - \{0\}$ , then the point  $x_0$  is a critical point of center-center type.*
- *If the spectrum has the form  $i\alpha, -i\alpha, \beta, -\beta$ , where  $\alpha, \beta \in \mathbb{R} - \{0\}$ , then the point  $x_0$  is a critical point of center-saddle type.*

- If the spectrum has the form  $\alpha + i\beta, \alpha - i\beta, -\alpha + i\beta, -\alpha - i\beta$ , where  $\alpha, \beta \in \mathbb{R} - \{0\}$ , then the point  $x_0$  is a critical point of focus-focus type.

We compute the spectrum of the linearization of the Hamiltonian vector field  $X_H$  with Hamiltonian (7) using Assertion 7.

ASSERTION 17. For all three series of critical points of rank 0 from Assertion 15 the spectrum of the linearization of the Hamiltonian vector field  $X_H$  with Hamiltonian (7) contains a zero eigenvalue with multiplicity 2. The spectrum also contains the following elements:

1. For the 1 series of critical points of rank 0 the spectrum also contains the eigenvalues  $\pm\sqrt{2}\sqrt{\alpha \pm \sqrt{\alpha^2 + 4\kappa\beta^2}}$ , where

$$\alpha = \kappa c_1^2 - J_1^2 - J_2^2 = (2\kappa c_1^2 - \frac{a}{\kappa})$$

$$\beta = c_1 J_2 = c_1^2 a - \kappa^2 c_1^4 - \frac{b^2}{\kappa}$$

2. For the 2 series the spectrum also contains the eigenvalues

$$\pm 2\sqrt{c_1(x_1 - \kappa c_1)} \quad \text{and} \quad \pm 2\sqrt{-J_1^2 + 2c_1 x_1 - \kappa c_1^2}$$

3. For the 3 series the spectrum also contains the eigenvalues

$$\pm 4iJ_3 \quad \text{and} \quad \pm \sqrt{2}\sqrt{J_1^2 - 2J_3^2 - \kappa c_1^2}$$

We further note that in order to prove the nondegeneracy of the points it suffices to verify that all the 4 eigenvalues of the operator  $A_H$  are not equal to 0 and that there exists  $\lambda \in \mathbb{R}$  such that the spectrum of the operator  $A_F$ , where  $F = K + \lambda H$ , has exactly 2 non-zero eigenvalues. Indeed, then the restrictions of the operators  $A_H$  and  $A_K$  are linearly independent since otherwise the spectrum of any linear combination is obtained from the spectrum of the operator  $A_H$  by a multiplication by a constant (it follows from Assertion 7). Moreover, there is no need to verify that all the eigenvalues of the operator  $A_H$  are distinct since in this case the spectrum of some linear combination  $H + \mu F$  has 4 different non-zero eigenvalues.

For the series 2 and 3 the required coefficient of proportionality  $\lambda$  has already been found in Assertion 8 (we can put  $\lambda = 2(\kappa c_1^2 - J_1^2)$  and  $\lambda = 0$  for the series 2 and 3 respectively). For the series 1 we can use the fact that  $k = \frac{\lambda^2}{4}$  for the critical points in the preimage of points of the parabolas (10) and (11) and formally put  $\lambda = \sqrt{\frac{k}{2}}$ . Then for the function  $F = K + \sqrt{\frac{k}{2}}H$  the spectrum of the operator  $A_F$  consists only of 4 zeroes and

$$\pm 4\sqrt{2}\sqrt{\frac{4\kappa b^2 - a^2}{\kappa^2} \left( \frac{a^2 - 2\kappa c_1^2}{\kappa} + \sqrt{\frac{a^2 - 4\kappa b^2}{\kappa^2}} \right)}.$$

It is now not hard to check the nondegeneracy of points from Lemmas 2 and 4. (Note that the degenerate points appear only at the boundaries of the areas of the plane  $\mathbb{R}^2(a, b)$  and their degenerations are related to the restructurization of the bifurcation diagrams in a neighbourhood of these points).

The types of critical points can be easily found using Assertions 16 and 17. Lemmas 2 and 4 are proved.  $\square$

#### 4.4 Proof of Theorems 1, 2 and 3

Theorems 1, 2 and 3 easily follow from earlier-proved Lemmas 1, 2, 3, 4 and the following simple geometric considerations.

1. First, we use the fact that the orbits of the coadjoint representation  $M_{a,b}$  of the Lie algebra  $\mathfrak{so}(4)$  are compact. In particular, since the image of a compact set is compact, it allows us to discard all unlimited domains during the construction of bifurcation diagrams.
2. Second, we use some well known results about nondegenerate singularities. All the required statements are described in detail in the book [4] so we only briefly recall them.
  - (a) There exists only one, up to Liouville equivalence, singular point of center-center type. The bifurcation diagram in a neighbourhood of a center-center singularity is the union of two curves emanating from this point. The loop molecule of the singularity has the form  $A - A$  and the mark  $r = 0$ .
  - (b) Any singularity of center-saddle type is Liouville equivalent to a direct product of a saddle atom and the elliptic atom  $A$ . In a neighbourhood of an image of a center-saddle point the bifurcation diagram is the union of a curve passing through this point and another curve emanating from this point. The loop molecule is obtained from the corresponding saddle atom by adding the atom  $A$  at the end of each edge, all marks  $r = \infty$ . (For example the loop molecule of the point  $y_{12}$  in Table 2 has such form.)
  - (c) There exists exactly 4 singularities of saddle-saddle type of complexity 1 (that is, containing exactly one singular point on the leaf). These singularities are completely determined by their loop molecules. (The required two loop molecules for the saddle-saddle singularities are given in Table 2 for the points  $y_3$  and  $y_7$ .)
3. Third, since we consider a two-parameter family of orbits  $M_{a,b}$  we can use the fact that some invariants of the system continuously depend on the parameters  $a$  and  $b$  (for example a small perturbation of the parameters does not change the number of tori in the preimage of regular points from the “same area”).

We also use stability of bifurcations of types  $A$ ,  $B$  and  $A^*$ .

In this section we do not consider the classical Kovalevskaya case ( $\varkappa = 0$ ) because it was considered earlier in the paper [10] and was described in detail in the book [4].

Also, we do not consider the case  $b = 0$  in much detail: the proof of the statements in this case is similar to the proof in the case  $b \neq 0$ .

of *Theorems 1 and 2*. Previously it was shown that the required bifurcation diagrams of the momentum mapping is contained in the union of curves described in Lemma 1. Therefore, to prove the theorems it remains to throw away several parts of the described curves and determine the bifurcations for the remaining arcs. Let us show how it can be done using the previously obtained information about the types of critical points of rank 0 (see Lemmas 2 and 4).

We prove Theorems 1 and 2 for the values of the parameters  $a$  and  $b$  from the area  $I$ , that is in the case  $|b| > \varkappa^{3/2}c_1^2$ ,  $2\sqrt{\varkappa}b < a < f_t(b)$  (where the function  $f_t(b)$  is given by the formula (15)). The remaining cases are treated similarly.

In this case the bifurcation diagram of the momentum mapping should have the form shown in Fig. 3, 4, 5. Denote by  $P$ ,  $Q$  and  $R$  the point of intersection of the curve (9) with the line  $k = 0$ , the point of intersection of the parabolas (10) and (11) and the point of intersection of the right parabola (11) with the line  $k = 0$  respectively.

First of all, we discard all unlimited domains (since the orbits of  $so(4)$  are compact) and all areas lying below the line  $k = 0$  (obviously,  $k \geq 0$ ). Then notice that the “curvilinear triangles”  $y_{12}y_{13}P$  and  $z_1z_2R$  do not belong to the image of the momentum mapping. Indeed, the point  $z_1$  is the rightmost point in the image of the coadjoint orbits because all the points in the preimage of the rightmost point on the line  $k = 0$  must be of center–center type and there is no images of critical points of rank 0 to the right of the point  $z_1$ . Similarly, if the point  $P$  belonged to the image of the momentum mapping, then it would be the leftmost and the lowest point in some of its neighbourhood. Therefore, there would have to be points of rank 0 in its preimage, which is false.

Further, since we know the types of all points of rank 0 we can easily determine the bifurcations corresponding to all arcs that contain an image of a critical points of rank 0. In this case the only ambiguity occurs for the point  $y_{10}$ . This point is the image of two points of center-center type thus a priori there are 3 variants: for the area lying to the left of the point  $y_{10}$  there are either 4, or 2 or 0 tori in the preimage. Let us show that only the first case is possible. If we increase the parameter  $a$ , then in the case  $f_t(b) < a < f_k(b)$  there appears the point  $y_7$  of saddle–saddle type, therefore there have to be 4 tori in the preimage of a point in the neighbouring camera. For the reasons of continuity in the case  $a < f_t(b)$  there should also be 4 tori for the camera to the left of the point  $y_{10}$ .

It remains to determine whether the “curvilinear triangle”  $y_8z_2Q$  and the arc  $y_8y_{13}$  belong to the bifurcation diagram and what bifurcations correspond to these arcs. The curve  $y_8Q$  does not belong to the bifurcation diagram, and the curve  $z_2Q$  belongs since in this case there is no critical points of rank 0 in the preimage of the point  $q$ . Here we use the following simple assertion.

**ASSERTION 18.** *Let  $(M^4, \omega)$  be a compact symplectic manifold,  $H, K$  be two commuting (with respect to the Poisson bracket) functions on  $M^4$ , which are independent almost everywhere. Suppose that in a neighbourhood of a point  $x \in \mathbb{R}^2$  the bifurcation diagram has the same structure as for the critical points of rank 0 of center–center type*

(that is, two arcs from the boundary of the image intersect transversely) or of center–saddle type (that is, an arc transversely intersects a smooth arc from the boundary of the image of the momentum mapping). There there is a critical point of rank 0 in the preimage of the point  $x$ .

It remains to show that the arcs  $y_{13}y_8$  and  $y_8z_2$  belong to the bifurcation diagram and that the corresponding bifurcations have types  $2B$  and  $2A^*$  respectively. Let us start with the arc  $y_8z_2$ . We already know (see Assertion 4) that the preimage of the points of this arc is either empty or consists of two critical circles and in the latter case the symmetry  $(J_3, x_3) \rightarrow (-J_3, -x_3)$  interchanges these circles. First of all we show that if the preimage consists of two critical circles, then the bifurcations corresponding to each of them have type  $A^*$ . Since there are two circles and they transform two tori into two and the system has a symmetry, the only possible bifurcation apart from  $2A^*$  is the bifurcation  $C_2$ . In order to show that the latter case can not occur let us consider the isoenergetic surfaces  $H = \text{const}$  for the values of energy  $H$  close to  $h_0 = \frac{b^2 c_1^2}{z_{rt}^2} + 2z_{rt}$ , where  $z_{rt}$  is given by the formula (37) (this value of energy corresponds to the point of tangency of the right parabola (11) and the parametric curve (9)). Since there is no points where the Hamiltonian vector field  $X_H$  vanishes for the values of  $H$  close to  $h_0$  the type of the isoenergetic surface does not change in a neighbourhood of  $h_0$ . However, when the energy parameter increases  $H > h_0$  the isoenergetic surface is obviously disconnected: its rough molecule consists of two copies of  $A - A$ . Therefore, it is disconnected for the lower values of  $H$  as well. However, if the bifurcation for the curve  $y_8z_2$  had type  $C_2$ , then the isoenergetic surface would have been connected. Thus the only bifurcation that can correspond to the curve  $y_8z_2$  is  $2A^*$ .

Now let us show that the bifurcations for the curve  $y_8z_2$  do really exist. First of all we notice that for sufficiently large values of the parameter  $a$  (more precisely, for  $a > f_m(b)$ ) these bifurcations exist (and they are of type  $2A^*$ ). It suffices to show that the loop molecule of the point  $y_3$  has the form shown in Table 2. It is true because there are 3 tori in the preimage of the points to the “left” of the point  $y_3$  and there are two tori in the preimage of the points to the “right”. It easily follows from the analysis of the types of critical points in the case  $f_r(b) < a < f_m(b)$  and in the case  $a > f_m(b)$  it follows from the reasons of continuity. Note that for  $a > f_m(b)$  the bifurcation for the arc  $y_3z_2$  has type  $2A^*$  since the critical point of rank 0 in the preimage of the point  $z_3$  has center–saddle type and hence the bifurcation for the curve  $y_3z_3$  has to be orientable.

From the reasons of continuity it follows that the bifurcations for the curve  $y_8z_2$  exist in case  $a < f_m(b)$ . Let us describe the last transition in more detail. On one hand, the bifurcations of the type  $A^*$  are stable, hence they survive under a small perturbation of parameters  $a$  and  $b$ . Therefore, the set of points  $a, b$  for which the bifurcation for the curve  $y_8z_2$  exists and has type  $2A^*$  is an open subset. On the other hand, the set of points where the Hamiltonian vector fields  $X_H$  and  $X_K$  are linearly dependent is a closed subset of  $\mathbb{R}^7 = \mathbb{R}^7(\mathbf{J}, \mathbf{x}, \varkappa)$ . Therefore, since the orbits of  $\text{so}(4)$  compact, the image of all critical points with  $\varkappa > 0$  by the mapping  $(H, K, a, b, \varkappa) : \mathbb{R}^7(\mathbf{J}, \mathbf{x}, \varkappa) \rightarrow \mathbb{R}^5$  is a closed set. Therefore, the set of points  $a, b$  for which the bifurcations for the curve  $y_8z_2$  exist is a closed subset. It follows that these bifurcations exist and have type  $2A^*$  for any value of the parameter  $a > 2\sqrt{\varkappa b}$  (and  $b^2 > \varkappa^3 c_1^4$ ).

Finally we prove that the bifurcation corresponding to the arc  $y_8y_{13}$  has type  $2B$ . The arc  $y_8y_{13}$  belongs to the bifurcation diagram because there are 4 tori over the “bottom” region and 2 tori over the “top” region. The number of tori in the areas can be easily found by a careful examination of the types of critical points of rank 0. For example, 2 tori lie over the “top” region since the point  $y_{12}$  is the image of a single point of center-saddle type and hence the bifurcation for the curve  $y_{12}z_5$  has type  $B$  (that is, one torus transforms into two).

We further note that the bifurcation corresponding to the arc  $y_8y_{13}$  consists of two identical parts. Moreover, the following statement holds, which follows easily from Assertion 4 and the fact that there is no images of the points of rank 0 in a neighbourhood of the point  $y_8$ .

**ASSERTION 19.** *The preimage of a sufficiently small neighbourhood of the singular point  $y_8$  consists of two connected components and the symmetry  $\sigma_3 : (J_3, x_3) \rightarrow (-J_3, -x_3)$  interchanges these components.*

Thus there are two identical bifurcations corresponding to the arc  $y_8y_{13}$ , which transform two tori into four. It follows from considerations of continuity as previously for the bifurcations  $2A^*$  that both these bifurcations have type  $B$ : for  $a > f_t(b)$  the bifurcation corresponding to the arc  $y_7y_8$  has type  $2B$  (the loop molecule of the saddle–saddle point in the preimage of the point  $y_7$  is uniquely determined by the fact that there are 4 tori in the preimage of points in one of the neighbouring cameras).

Thus we determined all the bifurcations. Theorems 1 and 2 are proved.  $\square$

*of Theorem 3.* The structure of loop molecules for nondegenerate singularities of rank 0 is well known and is described in detail in the book [4]. It remains to prove Theorem 3 for the images of degenerate critical points of rank 1. In almost all cases the loop molecules (without marks) for degenerate critical points can be uniquely determined using the obtained information about the bifurcations and the number of tori for all areas. Ambiguity for the loop molecules of points  $y_8$  and  $y_9$  can be easily solved using the fact that the loop molecules of these points must consist of two identical parts (see Assertion 19). Marks for the degenerate singularities can be found using standard methods (“rule of summation of the marks”, considerations of continuity), which are described, for example, in [4] or [21].  $\square$

## 5 Classical Kovalevskaya case ( $\varkappa = 0$ )

In this section we show that the bifurcation diagrams for classical Kovalevskaya case defined on the Lie algebra  $\mathfrak{e}(3)$  by the Hamiltonian

$$H = J_1^2 + J_2^2 + 2J_3^2 + 2x_1 \tag{44}$$

and the integral

$$K = (J_1^2 - J_2^2 - 2x_1)^2 + (2J_1J_2 - 2x_2)^2 \tag{45}$$

can be obtained from the bifurcation diagrams of the integrable Hamiltonian system with Hamiltonian (7) and the first integral (8) (where  $c_1 = 1$ ) on the Lie algebra  $\mathfrak{so}(4)$

by passing to the limit  $\varkappa \rightarrow 0$ . This limit  $\varkappa \rightarrow 0$  preserves types of critical points of rank 0, the bifurcations of Liouville tori and the loop molecules of singular points of the momentum mapping.

The structure of bifurcation diagrams for the classical Kovalevskaya case is well known and is described, for example, in [10] and [4]. However, in this section we not only compare the answers but also show how to construct the bifurcation diagram for the classical Kovalevskaya case and compute some of its invariants (more precisely, in this section we determine the bifurcations of Liouville tori) using the obtained information about the Kovalevskaya case on the Lie algebra  $so(4)$  while performing as little as possible additional calculations.

In this section we denote by  $\Sigma(a, b, 0)$  the bifurcation diagram of the momentum mapping for the orbit  $M_{a,b}$  of the Lie algebra for which the corresponding value of the parameter of the pencil is equal to  $\varkappa$ .

LEMMA 6. *Consider arbitrary  $a, b \in \mathbb{R}$  such that  $a > 0$ . Then a point  $x$  belongs to the bifurcation diagram  $\Sigma(a, b, 0)$  if and only if there exists a sequence of points  $x_n \in \Sigma(a_n, b_n, \varkappa_n)$  such that  $\lim_{n \rightarrow \infty} (a_n, b_n, \varkappa_n) = (a, b, 0)$ .*

*Proof.* In one direction, it follows from Assertion 2 that for any critical point  $z$  on the Lie algebra  $e(3)$  (that is, for a point with the parameter  $\varkappa = 0$ ) there exists a sequence of critical points  $z_n$  on the Lie algebra  $so(4)$  (that is, such that the value of the parameter  $\varkappa > 0$ ) converging to it. Therefore, the image of the point  $z$  is the limit of the images of points  $z_n$ .

In the other direction, the proof is by contradiction. Suppose that a point  $x \in \mathbb{R}^2$  is regular, that is  $x \notin \Sigma(a, b, 0)$ , but there exists a sequence  $x_n \in \Sigma(a_n, b_n, \varkappa_n)$  such that  $x_n \rightarrow x$  and  $(a_n, b_n, \varkappa_n) \rightarrow (a, b, 0)$  as  $\varkappa \rightarrow 0$ . In order to get a contradiction, we choose a point  $z_n$  in the preimage of each point  $x_n$  and prove that sequence  $z_n$  contains a convergent subsequence. To do this we show that the sequence  $z_n$  is contained in a compact set  $A \subset \mathbb{R}^7(\mathbf{J}, \mathbf{x}, \varkappa)$ .

Consider two sufficiently small closed discs  $\overline{D}_1$  and  $\overline{D}_2 \subset \mathbb{R}^2$  that contain points  $x$  and  $(a, b)$  respectively and a small segment  $[0, T] \subset \mathbb{R}$ . Then the set

$$A = \{(J, x, \varkappa) | (H, K, f_1, f_2, \varkappa)(\mathbf{J}, \mathbf{x}, \varkappa) \in \overline{D}_1 \times \overline{D}_2 \times [0, T]\}$$

is compact. Indeed,  $A \subset \mathbb{R}^7$  is a closed subset since  $\overline{D}_1 \times \overline{D}_2 \times [0, T]$  is a closed subset of  $\mathbb{R}^5$  and the mapping  $(H, K, f_1, f_2, \varkappa) : \mathbb{R}^7(\mathbf{J}, \mathbf{x}, \varkappa) \rightarrow \mathbb{R}^5$  is continuous. It remains to prove that the set  $A$  is bounded. Note that the set of numbers  $(x_1, x_2, x_3)$  is bounded since the integral  $f_1 = \varkappa \mathbf{J}^2 + \mathbf{x}^2$  is bounded above and below by some constants. It remains to note that the set of numbers  $(J_1, J_2, J_3)$  is also bounded because

$$J_1^2 + J_2^2 + 2J_3^2 = H - 2c_1 x_1$$

and the right side is bounded since  $(H, K) \in \overline{D}_1$  for all points from  $A$ . Lemma 6 is proved.  $\square$

It is not hard to get the exact equations for the curves that contain the bifurcation diagrams of the momentum mapping for  $\varkappa = 0$ . To do this it suffices to pass to the limit  $\varkappa \rightarrow 0$  in the equations for the curves (9) and (10) (the right parabola (11) “shifts to the right to infinity” as  $\varkappa \rightarrow 0$  thus it has no limit points for  $\varkappa = 0$ ).

LEMMA 7. Let  $\varkappa = 0$  and  $b \neq 0$ . Then for any non-singular orbit  $M_{a,b}$  (that is, for any orbit such that  $a > 0$ ) the bifurcation diagram  $\Sigma_{h,k}$  for the integrable Hamiltonian system with Hamiltonian (7) and integral (8) is contained in the union of the following three families of curves on the plane  $\mathbb{R}^2(h, k)$ :

1. The line  $k = 0$ ;
2. The parametric curve

$$h(z) = \frac{b^2 c_1^2}{z^2} + 2z, \quad k(z) = 4ac_1^2 - \frac{4b^2 c_1^2}{z} + \frac{b^4 c_1^4}{z^4}, \quad (46)$$

where  $z \in \mathbb{R} - \{0\}$ .

3. The parabola

$$k = \left( h - \frac{2b^2}{a} \right)^2. \quad (47)$$

We have an analogous statement for  $b = 0$ .

LEMMA 8. Let  $\varkappa = 0$  and  $b = 0$ . Then for any non-singular orbit  $M_{a,0}$  (that is, for any orbit such that  $a > 0$ ) the bifurcation diagram  $\Sigma_{h,k}$  for the integrable Hamiltonian system with Hamiltonian (7) and integral (8) is contained in the union of the following three families of curves on the plane  $\mathbb{R}^2(h, k)$ :

1. The line  $k = 0$ ;
2. The union of the parabola

$$k = h^2 + 4ac_1^2 \quad (48)$$

and the tangent line to this parabola at the point  $h = 0$

$$k = 4ac_1^2. \quad (49)$$

3. The parabola

$$k = h^2. \quad (50)$$

Now we determine which areas described in Theorems 1 and 4 survive as  $\varkappa \rightarrow 0$ . It is not hard to check that in the limit the curves  $f_k, f_r, f_t$  and  $f_l$  given by the formulas (12), (13), (15) and (16) respectively go to the curves  $a = \frac{3}{4} \frac{b^{4/3}}{c_1^{2/3}}$ ,  $a = \frac{b^{4/3}}{c_1^{2/3}}$ ,  $a = \frac{1}{2^{2/3}} \frac{b^{4/3}}{c_1^{2/3}}$  and  $b = 0$  respectively. (For a fixed  $b \neq 0$  the curve  $f_m(b)$  has no limit points in the area  $\{a > 0, b > 0\}$  as  $\varkappa \rightarrow 0$ .) The found curves divide the area  $\{a > 0, b > 0\}$  into 4 sub-areas which we denote in this paper as follows:

1. Area I' is the area  $\{\varkappa = 0, \quad 0 < b, \quad 0 < a < \frac{1}{2^{2/3}} \frac{b^{4/3}}{c_1^{2/3}}\}$ ;
2. Area II':  $\{\varkappa = 0, \quad 0 < b, \quad \frac{1}{2^{2/3}} \frac{b^{4/3}}{c_1^{2/3}} < a < \frac{3}{4} \frac{b^{4/3}}{c_1^{2/3}}\}$ ;
3. Area III' :  $\{\varkappa = 0, \quad 0 < b, \quad \frac{3}{4} \frac{b^{4/3}}{c_1^{2/3}} < a < \frac{b^{4/3}}{c_1^{2/3}}\}$ ;

4. Area IV':  $\{\varkappa = 0, \quad 0 < b, \quad \frac{b^{4/3}}{c_1^{2/3}} < a\}$ .

If  $\varkappa = 0$ , then all the curves  $f_r, f_k, f_t$  and  $f_l$  intersect only at the origin, therefore in this case we should consider only one additional area of the line  $b = 0$ :

1. Area V':  $\{\varkappa = 0, \quad b = 0, \quad 0 < a\}$ .

REMARK 11. If  $\varkappa = 0$ , then without loss of generality, we can assume that  $a = 1$  (other orbits can be obtained from the case  $a = 1$  by a suitable change of variables). It is not hard to check that the line  $a = 1$  intersects the areas I'–V' at the following subsets: it intersects the first four areas at the intervals  $2 < b^2, (4/3)^{3/2} < b^2 < 2, 1 < b^2 < (4/3)^{3/2}$  and  $0 < b^2 < 1$  (intervals are listed in ascending order of areas) and it intersects the area V' at the point  $b = 0$ .

Now it is not hard to understand how the bifurcation diagrams for the classical Kovalevskaya case look like: roughly speaking, they are obtained from the diagrams shown in Fig. 3–14 (or in Fig. 22 for  $b = 0$ ) by removing all the “right arcs”, that is all the arcs belonging to the right parabola (11) and the arc  $z_1 z_2$ . Namely, the following theorem holds.

THEOREM 5 ([10]). *Let  $\varkappa = 0$  and  $b > 0$ . The curves*

$$a = \frac{b^{4/3}}{c_1^{2/3}}, \quad a = \frac{3b^{4/3}}{4c_1^{2/3}} \quad \text{and} \quad a = \frac{1}{2^{2/3}} \frac{b^{4/3}}{c_1^{2/3}}$$

*divide the area  $\{a > 0, b > 0\}$  into 4 areas. In Fig. 27–30 the bifurcation diagrams of the momentum mapping for the integrable Hamiltonian system with Hamiltonian (7) and integral (8) on the orbit  $M_{a,b}$  of the Lie algebra  $e(3)$  are shown for each of these areas. The enlarged fragments of Fig. 27, 28, 29 and 30 have the same forms as Fig. 14, 11, 8 and 5 respectively. The bifurcations diagram for the orbit  $M_{a,0}$  of the Lie algebra  $e(3)$  (that is, in the case  $\varkappa = 0, b = 0, a > 0$ ) is shown in Fig. 26.*

REMARK 12. In Fig. 27–30 the arcs  $y_1 y_2, y_2 y_3, y_3 y_5, y_2 y_7, y_7 y_8, y_1 y_{12}, y_{12} y_{13}$  and  $y_{13} y_8$  belong to the parabola (47). The rest of the arcs distribute between the curve (46) and the line  $k = 0$  in an obvious way.

*of Theorem 5.* First of all, it is necessary to check the nondegeneracy of the critical points in the case  $\varkappa = 0$  since in general critical points may become degenerate during a variation of parameters (for example, for the integrable system on the Lie algebra  $so(4)$  under consideration this happens when passing from one area of parameters  $a, b$  to another). Nevertheless, all calculations done in Sections 4.1 and 4.3 for the points of rank 1 and 0 respectively remain valid in the case  $\varkappa = 0$ , therefore it is not hard to verify that all critical points corresponding to non-singular points of the bifurcation diagram are nondegenerate critical points of rank 1 and that all critical points of rank 0 are nondegenerate and have the same type as the corresponding critical points of rank 0 for the Lie algebra  $so(4)$ .

Furthermore, it follows from the reasons of continuity that the preimage of each regular point in the image of the momentum mapping for the Lie algebra  $e(3)$  must

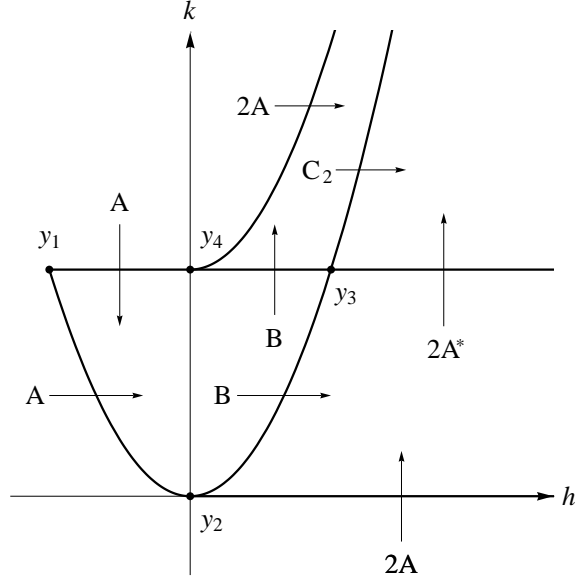


Figure 26: Classical Kovalevskaya case:  $\varkappa = 0, \quad b = 0$

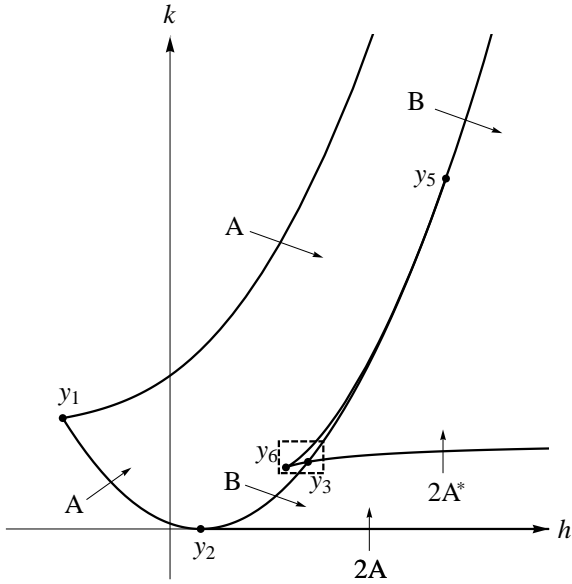


Figure 27: Classical Kovalevskaya case:  $\varkappa = 0, \quad a = 1, \quad 0 < b^2 < 1$

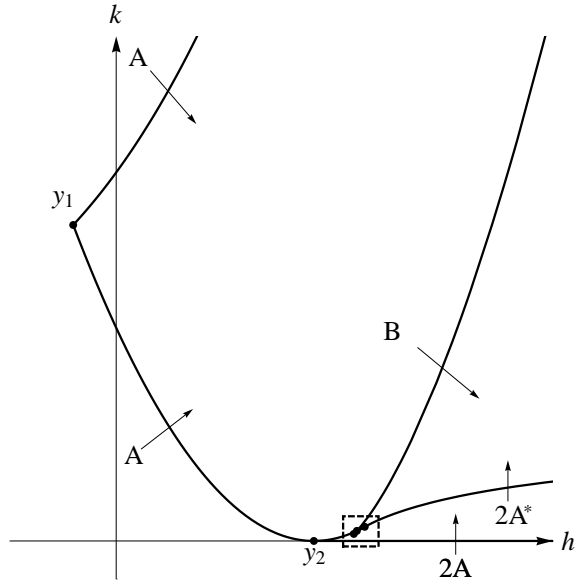


Figure 28: Classical Kovalevskaya case:  $\varkappa = 0, \quad a = 1, \quad 1 < b^2 < (4/3)^{3/2}$

contain the same number tori as the preimage of a regular point from the corresponding region for the Lie algebra  $so(4)$ . Similarly, the number of critical circles in the preimage of non-singular points of bifurcation diagrams must coincide. (The number of critical circles does not decrease because all singularities are nondegenerate. Under a small perturbation of parameters a complex singularities can decompose into several simple ones but it does not occur in this case — it follows from the explicit form of the bifurcation diagrams. The number of critical circles does not increase for the same arguments as in the proof of the fact in Lemma 6 that there is no points of bifurcation

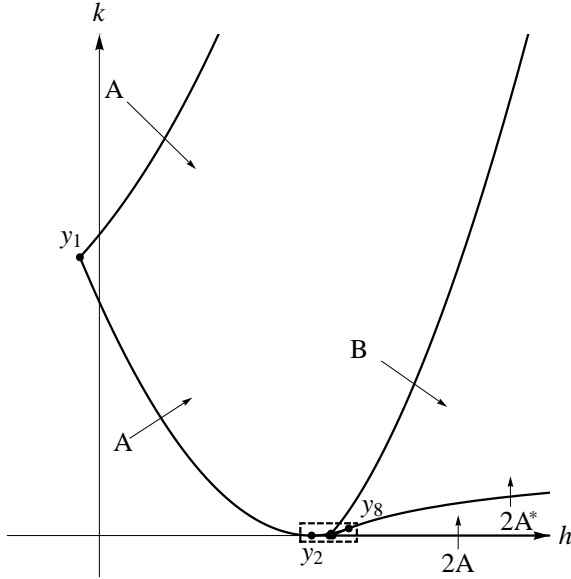


Figure 29: Classical Kovalevskaya case:  $\varkappa = 0$ ,  $a = 1$ ,  $(4/3)^{3/2} < b^2 < 2$

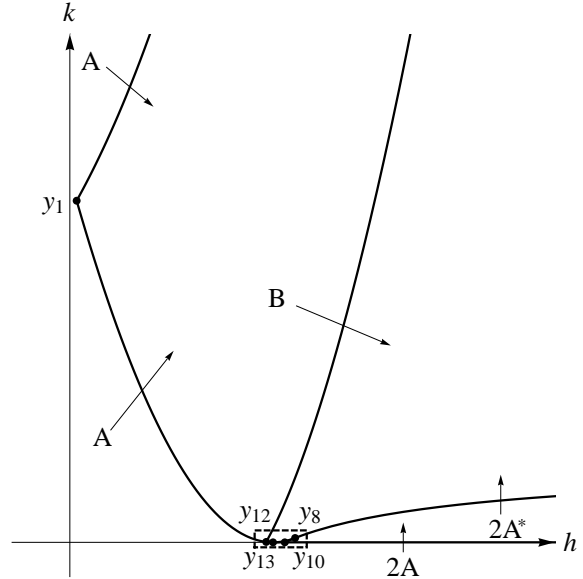


Figure 30: Classical Kovalevskaya case:  $\varkappa = 0$ ,  $a = 1$ ,  $2 < b^2$

diagrams in a neighbourhood of a regular point).

Now, since we know the types of critical points of rank 0, the numbers of tori and critical circles we can determine almost all bifurcations of Liouville tori. It remains to use the stability of bifurcations  $A$ ,  $B$  and  $A^*$  and standard considerations of continuity to get rid of the ambiguity for some arcs. For example, in the case  $\varkappa = 0, b = 0$  the bifurcation corresponding to the arc  $P_1$  has type  $C_2$  and not  $2A^*$  since the bifurcation corresponding to the arc  $y_3z_5$  has type  $C_2$ .

Theorem 5 is completely proved. □

## References

- [1] S. Kowalewski, “Sur une propriété du système d’équations différentielles qui définit la rotation d’un corps solide autour d’un point fixe”, *Acta Mathematica*, **14**:1 (1890), 81-93.
- [2] S. Kowalewski, “Sur le problème de la rotation d’un corps solide autour d’un point fixe”, *Acta Mathematica*, **12**:1 (1889), 177–232.
- [3] I. V. Komarov, “Kowalewski basis for the hydrogen atom”, *Teoret. Mat. Fiz.*, **47**:1 (1981), 67–72; English transl. in *Theoret. and Math. Phys.* **47**:1 (1981), 320–324.
- [4] A. V. Bolsinov, A. T. Fomenko, *Integrable Hamiltonian systems. Geometry, topology, classification*, vols. 1,2, Udmurtian University Publishing House, Izhevsk 1999, 444 p., 447 pp.; English transl., Chapman & Hall/CRC, Boca Raton, FL 2004, xvi+730 pp.

- [5] A. A. Oshemkov, “The topology of surfaces of constant energy and bifurcation diagrams for integrable cases of the dynamics of a rigid body on  $SO(4)$ ”, *Uspekhi Mat. Nauk* **42**:6(258) (1987), 199–200; English transl. in *Russian Math. Surveys* **42**:6 (1987), 241–242.
- [6] G. Haghghatdoost, A. A. Oshemkov, “The topology of Liouville foliation for the Sokolov integrable case on the Lie algebra  $so(4)$ ”, *Mat. Sb.* **200**:6 (2009), 119–142; English transl. in *Sb. Math.* **200**:6 (2009), 899–921.
- [7] H. Khorshidi, “The topology of an integrable Hamiltonian system for the Steklov case on the Lie algebra  $so(4)$ ”, *Vestn. Mosk. Univ. Ser. 1 Mat. Mekh.*, 2006, no. 5, 58–61; English transl. in *Moscow Univ. Math. Bull.* **61**:5 (2006), 40–44.
- [8] A. S. Mishchenko, A. T. Fomenko, “Euler equations on finite-dimensional Lie groups”, *Izv. Akad. Nauk SSSR Ser. Mat.* **42**:2 (1978), 396–415; English transl. in *Math. USSR-Izv.* **12**:2 (1978), 371–389.
- [9] A. T. Fomenko, “Topological invariants of Liouville integrable Hamiltonian systems”, *Funktsional. Anal. i Prilozhen.* **22**:4 (1988), 38–51; English transl. in *Funct. Anal. Appl.* **22**:4 (1988), 286–296.
- [10] M. P. Kharlamov, *Topological analysis of integrable problems of rigid body dynamics*, Leningrad University Publishing House, Leningrad 1988, 200 pp. (Russian)
- [11] M. P. Kharlamov, “Bifurcation of common levels of first integrals of the Kovalevskaya problem”, *Prikl. Mat. Mekh.* **47**:6 (1983), 922–930; English transl. in *J. Appl. Math. Mech.* **47**:6 (1985), 737–743.
- [12] M. P. Kharlamov, “Topological analysis of classical integrable systems in the dynamics of a rigid body”, *Dokl. Akad. Nauk SSSR* **273**:6 (1983), 1322–1325; English transl. in *Soviet Math. Dokl.* **28**:3 (1983), 802–805.
- [13] A. V. Bolsinov, P. H. Richter, A. T. Fomenko, “The method of loop molecules and the topology of the Kovalevskaya top”, *Mat. Sb.* **191**:2 (2000), 3–42; English transl. in *Sb. Math.* **191**:2 (2000), 151–188.
- [14] I. K. Kozlov, T. S. Ratiu, “A bifurcation diagram for the Kovalevskaya case on the Lie algebra  $so(4)$ ”, *Dokl. Ross. Akad. Nauk* **447**:5 (2012), 486–489; English transl. in *Dokl. Math.* **86**:3 (2012), 827–830.
- [15] A. V. Borisov, I. S. Mamaev, *Modern methods of the theory of integrable systems*, Contemporary Mathematics, Institute of Computer Studies, Moscow–Izhevsk 2003, 296 pp. (Russian)
- [16] A. T. Fomenko, “Symplectic topology of integrable dynamical systems. Rough topological classification of classical cases of integrability in the dynamics of a heavy rigid body”, *Differential geometry, Lie groups and mechanics*. 15–2, Zap. Nauchn. Sem. St.-Peterburg. Otdel. Mat. Inst. Steklov., vol. 235, St.-Peterburg. Otdel.

Mat. Inst. Steklova, St.-Petersburg 1996, pp. 104–183; *J. Math. Sci. (New York)* **94**:4 (1999), 1512–1557.

- [17] E. A. Kudryavtseva, I. M. Nikonov, A. T. Fomenko, “Maximally symmetric cell decompositions of surfaces and their coverings”, *Mat. Sb.* **199**:9 (2008), 3–96; English transl. in *Sb. Math.* **199**:9 (2008), 1263–1353.
- [18] A. T. Fomenko, A. Yu. Konyaev, “New approach to symmetries and singularities in integrable Hamiltonian systems”, *Topology Appl.* **159**:7 (2012), 1964–1975.
- [19] E. A. Kudryavtseva, A. T. Fomenko, “Symmetries groups of nice Morse functions on surfaces”, *Dokl. Ross. Akad. Nauk* **446**:6 (2012), 615–617; English transl. in *Dokl. Math.* **86**:2 (2012), 691–693.
- [20] A. T. Fomenko, E. A. Kudryavtseva, “Each finite group is a symmetry group of some map (an ‘Atom’-bifurcation)”, *Vestn. Moskov. Univ. Ser. 1 Mat. Mekh.* **67**:3 (2013), 21–29; English transl., *Moscow Univ. Math. Bull.* **68**:3 (2013), 148–155.
- [21] P. V. Morozov, *Fine Liouville classification of some integrable cases in rigid body mechanics*, Kandidat Thesis, Faculty of Mechanics and Mathematics, Moscow State University, Moscow 2006, 170 pp. (Russian)